Local-scale post-event assessments with GPS and UAV-based quick response surveys: a pilot case from the Emilia-Romagna (Italy) coast

Enrico Duo[1], Arthur C. Trembanis[2], Stephanie Dohner[2], Edoardo Grottoli[1], and Paolo Ciavola[1]

[1] Department of Physics and Earth Sciences, University of Ferrara
[2] School of Marine Science and Policy, University of Delaware

Correspondence to: Enrico Duo (enrico.duo@unife.it)

Abstract. Coastal communities and assets are exposed to flooding and erosion hazards due to extreme storm events, which may increase in intensity due to climatological factors in the incoming future. Coastal managers are tasked with developing risk management plans mitigating risk during all phases of the disaster cycle. This necessitates rapid, time-efficient post-event beach surveys to collect physical data in the immediate aftermath of an event. Additionally, the inclusion of local stakeholders in the assessment process via personal interviews captures the social dimension of the impact of the event. In this study, a local protocol for post-event assessment, the Quick Response Protocol, was tested on a pilot site on the Emilia-Romagna (Italy) coast in the aftermath of an extreme meteorological event occurred in February 2015. Physical data were collected using both Real-Time Kinematic Geographical Positions Systems and Unmanned Aerial Vehicle platforms. Local stakeholders were interviewed collecting qualitative information on their experiences before, during and after the event. Data comparisons between local and regional surveys of this event highlighted higher data resolution and accuracy at the local level, enabling improved risk assessment for future events of this magnitude. The local survey methodology, although improvable from different technical aspects, can be readily integrated into regional surveys for improved data resolution and accuracy of storm impact assessments on the regional-scale to better inform coastal risk managers during mitigation planning.

1 Introduction

Extreme storm events have the potential to produce coastal flooding and erosion, reshape coastlines, impact infrastructures, and expose populations to hazardous conditions. The most damaging events consist of a combination of extreme wave heights, storm surge, wind direction, and tidal stage that interact with the morphology of the beach and adjacent infrastructures generating direct and indirect impacts (Van Dongeren et al., 2018; Viavattene et al., 2018). Given the expectation of increasing storm intensities and occurrence (Bason et al., 2007), accurate and rapid field data collection must occur to best inform risk management and policy decisions (Casella et al., 2016). To ensure that appropriate (risk) management plans are implemented, precise and high-resolution field measurements are crucial to understand storm effects on exposed communities, providing input datasets for numerical modelling for future event impacts (Lee et al., 1998; Stone et al., 2004; Nicholls et al., 2007).

Additionally, the inclusion of local stakeholder interviews is essential to appropriately address group values, create risk reduction plans supported by locals, and implement proposed plans within the community (Martinez et al., 2018). Coastal managers must determine which management protocols are appropriate during all phases of the risk cycle including prevention, preparedness, response and recovery while balancing needs at local, regional, and country scales. Europe recognizes the value of standardized protocols for risk management as an effective way to coordinate field efforts, improve hazard maps, and enhance risk reduction plans (Poljanšek et al., 2017).

However, post-storm assessments require capturing the morphologic signature of the event using rapid, quantitative mapping as soon as safe conditions allow following the event but before recovery processes begin (i.e. natural or human-driven) (Morton et al., 1993; Bush et al., 1999; Morton, 2002). This data can be difficult to obtain as traditional post-storm survey techniques are expensive or time-consuming on large scales. To properly quantify impacts, pre-storm quantitative mapping of the area is necessary before impacts can be attributed to a single storm. In recent years, autonomous platform methodologies for coastal mapping and extreme event impact assessment were proposed and tested to improve traditional, expensive, or time-consuming mapping approaches on both the emergent beach (Mancini et al., 2013; Casella et al., 2016; Turner et al., 2016) and the submerged nearshore area (Trembanis et al., 2013).

Real-Time Kinematic Geographical Positions Systems (RTK GPS) for ground-based surveys (Morton et al., 1993; Theuerkauf and Rodriguez, 2012) are the traditional method for topographic data requiring highly accurate (sub-decimeter) positioning measurements. These systems are utilized in the coastal environment for temporal and spatial monitoring of many coastal morphologic features through periodic monitoring and post-event surveys (Larson and Kraus, 1994; Benedet et al., 2007; Hansen and Barnard, 2010; Theuerkauf and Rodriguez 2012). Since the sampling point density of the RTK GPS survey affects the accuracy of beach morphology representation, insufficient resolutions (e.g. representing the beach with traditional profile spacings of more than 100 meters) can lead to imprecise or misleading morphological interpretations of storm impacts (Swales, 2002; Berstein et al., 2003; Pietro, et al., 2008; Theuerkauf and Rodriguez, 2012). The ideal resolution of the RTK GPS survey depends on the scale of the study and on its location. Terrestrial laser scanners or total stations improve point density but require similar time and physical effort as RTK GPS, particularly when surveying large areas (Saye et al., 2005; Theuerkauf and Rodriguez, 2012; Lee et al., 2013). Improvements in remote sensing technology have increased data resolution through airborne lasers (LiDAR) and satellite imagery but the high costs of operations and infrequent surveys render these options impractical for local scales and rapid or frequently repeated surveys (Stockdon et al., 2002; Young and Ashford, 2006; Anderson and Gaston, 2013). Phillips et al. (2017) proposed a high-frequency LiDAR surveying methodology by fixing a laser system to a housing structure on a beach to continuously measure topographic profiles. The system provided unique, temporally dense morphological recovery results but only of a single cross-shore profile thereby limiting the scope of data and ignoring the varied, three-dimensionality of coastal response.

Unmanned Aerial Vehicles (UAVs), known informally as “drones”, attempt to address temporal and spatial sampling issues at local scales thanks to rapid deployment, economic feasibility, and high-resolution, accurate topographic data when monitoring hydro-morphological changes in the coastal zone (Berni et al., 2009; Westoby et al., 2012; Casella et al., 2016;

James et al., 2017). Moloney et al. (2017) compared surveying methods for coastal dune monitoring in New Zealand and concluded that, compared to total station, RTK GPS and terrestrial laser scanner methods, the UAVs proved to be the cheapest option while being more accurate than total station and RTK GPS methods. The UAVs resulted ideal to monitor short- and long-term coastal dune systems with elevation data and aerial images. Seymour et al. (2017), compared terrestrial laser scanner and UAV, equipped with a RTK GPS system, for coastal monitoring and management in North Carolina (US). This study provided additional insights for field implementation and post-processing, including limitations of UAV data related to the environment (e.g. texture of the surveyed surface, solar angle, etc.). The study presented specific operational guidelines and demonstrated that UAVs provide affordable, frequent coastal environment monitoring at the local scales.

Beyond the pure physics of coastal risk management lies the often overlooked and unquantified social dimension of the local community affected daily by these hazards and management plans. Previous researchers documented that inclusion of local communities in assessing coastal risk and creating reduction plans, improves the quality of the plans while having a positive feedback on the population, through increased risk awareness and preparedness (Pescaroli and Magni, 2015; Becu et al., 2017; Gray et al., 2017; Martinez et al., 2018). In this sense, performing interviews of local people in the immediate aftermath of a coastal extreme event provides important information on the local evolution of the storm, on the effectiveness of the implemented emergency preparedness, and response phases (Martinez et al., 2018).

Building upon the foundations of the aforementioned work, this study presents a pilot field case focused on applying a quick response methodology for local post-storm coastal change assessment. This method relies on a combination of traditional RTK GPS surveys coupled with UAV aerial imagery, and qualitative data (i.e. interviews of local stakeholders). The aim of combining these approaches is creation of a rapid and holistic coverage of the field site and storm event. Implementation of the assessment approach was carried out in the Emilia-Romagna region of Italy. At the regional level, managers have adopted effective protocols for coastal risk management, early warning system and post-storm hazard and risk assessments (Ligorio et al., 2012; Perini et al., 2015b, 2016). The pilot study of the current paper demonstrates how the proposed approach provides local-scale high-resolution data capable of capturing individual storm-induced coastal changes. Furthermore, this integrated approach provides detailed insights into physical and social aspects that can be applied at the local, as well as at regional and national levels, for effective, coordinated cross-disciplinary management purposes.

2 Case study

2.1 Regional settings and study site

Regional Settings

A stretch of approximately 7 km of coast within the Ferrara province (Emilia-Romagna region), located on the Italian side of the Northern Adriatic Sea (Figure 1A, B), was surveyed immediately following an extreme (low-frequency and high-impact)

storm event (hereafter called the Saint Agatha storm; see Section 2.3) that occurred on 5-7 February 2015. The coastal landscape in Emilia-Romagna is generally comprised of low-lying sandy beaches with limited topographically elevated areas usually in the form of either relict beach ridges or artificial embankments (Armaroli et al., 2012). The shore is comprised of alternating spaces of natural areas with native dunes intermixed with urbanized areas consisting of buildings, roads, and walkways. Much of the sandy coast is currently occupied by tourist facilities, residential buildings, and bathing structures, as consequence of 60 years of continuous development and urbanization upon relict coastal ridges (Sytnik and Stecchi, 2014). Touristic beaches contain private concessions (i.e. properties located on public beach areas, granted to private individuals for commercial/tourism activities) that provide sun-and-bath and food services since the 1970s. Immediately behind the concessions, small residential towns developed and nowadays accommodate many second homes, hotels, and restaurants. These factors combine to increase the area's exposure to coastal hazards (i.e. flooding and erosion), particularly in the Ferrara and Ravenna provinces, where some elevations are below Mean Sea Level (MSL) (Perini et al., 2010). Since the end of World War II, a sediment deficit has affected the littoral budget due to decreased sediment transport load of local rivers, mainly caused by anthropogenic controls on the rivers and their basins (Preciso et al., 2012) and the reforestation of the Apennines (Billi and Rinaldi, 1997). This problem has been exacerbated over the last several decades by land subsidence, most likely caused by groundwater and gas extraction activities (Teatini et al., 2005; Taramelli et al., 2015). These issues prompted action in the form of defence structures (groins, breakwaters, etc.) being built along the coast in an effort to mitigate shoreline retreat due to sediment starvation (Armaroli et al., 2012).

The wave climate for the region is dominated by low wave energy (mean Hs ≈ 0.4 m, Tp ≈ 4 s) with a semidiurnal microtidal regime (neap tidal range= 0.30 m; spring tidal range = 0.8 m). Storm significant wave heights with a 1-year return period range up to 3.3 m (Armaroli et al., 2009) and storm surges with a 2-year return period reach up to 0.6 m (Masina and Ciavola, 2011). These storm events mainly occur in the fall and winter months (October-March). Storms are mainly characterized by ENE waves associated with Bora (NE) winds or by SE waves when caused by Scirocco (SE) winds. Storm surge events predominantly occur during Scirocco winds, which coincide with the main SE–NW orientation of the Adriatic Sea. Bora storm waves are generally large and steep, whereas Scirocco waves are smaller in height but with a longer wave period due to the increased fetched of lower winds speeds across the Adriatic (Harley et al., 2016).

Several methods for storm characterization have been developed and implemented in recent years for the Mediterranean coast. Mendoza et al., (2011) proposed a five-class intensity scale, defining a storm as an event in which the significant wave height exceeds 1.5 m for at least 6 hours (Mendoza and Jiménez, 2006). Moving to a more local perspective, Armaroli et al. (2012) adopted the same physical definition of storm events for the northern Adriatic Sea. Two storms are considered independent when the significant wave height decreases below the 1.5 m threshold for 3 or more consecutive hours. By analysing the events and their impacts together, Armaroli et al. (2012) classified a storm as "potentially damaging" when it exceeds the critical wave and total water level (TWL = surge + tide) thresholds of: Hs>=2m and TWL>=0.7m for urbanized beaches; Hs>=3.3m and TWL>=0.85m for natural beaches.

Case study site and target area

The pilot case study site is located between Porto Garibaldi and Lido di Spina and is characterized by highly urbanized, low-lying sandy beaches, with touristic concessions (concrete and/or wood buildings) directly facing the sea. The width of the beach ranges from ~20 m to ~150 m. The predominant sediment transport (longshore drift) is directed northward. The southern jetty of the canal harbour (Porto Canale) in Porto Garibaldi traps longshore sediment, resulting in widening of the beach at Lido degli Estensi and erosion of the Porto Garibaldi beach. Erosion appears again in the southern part of Lido di Spina (Nordstrom et al., 2015), as shown in Figure 1D. The southernmost concession at Lido di Spina defines the southern boundary of the case study. In the whole area, the concessions are affected by coastal storm impacts during extreme events (Nordstrom et al., 2015). The pilot case study site presents areas known as coastal risk prone at the regional level (Perini et al., 2016; Armaroli and Duo, 2018; Sanuy et al., 2018). The main analysis focuses on the target area on the southernmost portion of the beach at Lido degli Estensi (Figure 1E) in the municipality of Comacchio, east of Ferrara and north of Ravenna.

Figure 1. Field study site locations: A) Emilia-Romagna region; B) Coastal regional domain; C) Locations of the nearest tide gauge and wave buoy; D) Pilot case study site; E) Target area for data comparison.

2.2 Coastal alerts and monitoring in Emilia-Romagna

The Emilia-Romagna Region (RER) developed a protocol for coastal storm alert and monitoring, within the framework of a wider system for hydro-geological risk alert, and a conglomerate of agencies and regional services are involved in the process (Ligorio et al., 2012). The daily forecasting of waves, surge and coastal impacts, provided by the Servizio IdroMeteoClima of the Agenzia Regionale per la Prevenzione, l'Ambiente e l'Energia (ARPAE-SIMC) are evaluated, along with the weather forecast, by the regional geological service (Servizio Geologico Sismico e dei Suoli, SGSS), the Centro Funzionale of ARPAE (ARPAE-CF), the regional Servizio Difesa del Suolo della Costa e Bonifica (SDSCB), the technical services (Servizi Tecnici di Bacino, STB), the inter-regional agency of the Po river (Agenzia Interregionale Fiume Po, AIPO) and the Civil Protection. The forecasting of coastal hazards and impacts is provided through the Emilia-Romagna Early Warning System (E-R EWS), developed in the framework of the EU FP7 MICORE project (www.micore.eu), with the objective to predict the imminent arrival of a storm as a tool to be used by Civil Protection agencies and local communities (Ciavola et al., 2011; Harley et al., 2012, 2016; Jiménez et al., 2017). The E-R EWS is operational and maintained by ARPAE-SIMC and the University of Ferrara (UNIFE) through daily running of a sequence of numerical models (COSMO, SWAN, ROMS, and XBeach). The model chain aims to reproduce the hydro-morphodynamic response of the beach for 22 representative cross-shore profiles distributed along the regional coast. The final output of the chain is transformed into a format suitable for decision-makers and end-users (Harley et al., 2012). The EWS tool is based on Storm Impact Indicators (SIIs) (Ciavola et al., 2011) focusing on the magnitude of

water ingression and type of exposed assets, which are described as natural or urbanized beaches (Harley et al., 2016). The daily outputs are published on-line at http://geo.regione.emilia-romagna.it/schede/ews/.

From 2017, the RER activated an on-line portal (https://allertameteo.regione.emilia-romagna.it/) where the alerts are published in a GIS-based interface. In case of forecasted over-threshold events, or unexpected ones, the alert is issued to the Civil Protection who forwards it to the local technical services and municipalities. At this point, the monitoring phase begins, and updates are issued based on further observations (i.e. waves, water levels, wind, rains, etc.) and forecasting updates. If necessary, the emergency response is activated and implemented by the Civil Protection.

The SGSS oversees data collection and elaboration for coastal risk management purposes (Perini et al., 2015b; Armaroli and Duo, 2018). The geological service collects all available information from forecasting, observations, on-line pictures, webcam movies and news during and after a coastal event. After significant coastal events, the STBs are activated and implement on the ground surveys, documenting local impacts and measuring the water ingression. The SGSS also surveys (with DGPS techniques) 18 beach profiles in 13 locations along the coast, belonging to the regional beach monitoring network. After particularly damaging events, the Civil Protection flies over the impacted areas taking oblique aerial pictures. However, this is not a regular procedure and is infrequently implemented. All the information is elaborated and archived by the SGSS in the public GIS-based coastal information system (Sistema Informativo del Mare e della Costa, SIC; http://ambiente.regione.emilia-romagna.it/geologia/temi/costa/sistema-informativo-del-mare-e-della-costa-sic), in the in_Risk and in_Storm platforms (Perini et al., 2015b).

2.3 Storm event

During the period 5-7 February 2015, an extreme storm hit the Emilia-Romagna coast and the whole of the Northern Adriatic Sea, causing extensive flooding of urban and natural areas. The storm occurred in extreme regional weather conditions, which included heavy snow in the Apennines and rain in the alluvial plain of the Emilia-Romagna (ARPA E-R SIMC, 2015; Perini et al., 2015a, 2015b). The recorded water level was collected from the tide gauge of ISPRA (Istituto Superiore per la Protezione e la Ricerca Ambientale) located in Porto Corsini, Ravenna (Figure 1C). Wave data was recorded by the ARPA-ER (Agenzia Regionale per la Prevenzione e l'Ambiente dell' Emilia-Romagna) offshore wave buoy located at 10 m depth, 5.5 km offshore from the town of Cesenatico. The event, here referred to by the colloquial name of the Saint Agatha storm, was identified following the Armaroli et al. (2012) storm definition. It began at night and lasted for 51 hours, making it one of the longest duration storms recorded by the local wave buoy offshore of Cesenatico (Figure 1C) since its deployment in May 2007. The maximum water level (surge + tide) of 1.20 m was measured at 23:40 GMT on 5 February. The non-tidal residual time-serie was assessed based on tidal predictions (calculated for Porto Corsini using data for the period 2007-2015 with t_tide; Pawlowicz et al., 2002) and showed a peak of 1.27 m in the morning of 6 February (Figure 2). The skew surge for the tidal cycle that included the peak of the total water level was calculated and resulted in 0.92 m. The significant wave height (4.6 m)

and period (9.9 s) at the peak were recorded in the morning of 6 February (Figure 2). The wave direction was consistently from the ENE sector for the entire event duration.

According to the Mediterranean storm classification of Mendoza et al. (2011), the Saint Agatha storm is assigned to the severity class IV ("Severe"). The storm consequences were magnified by the combination of high waves, high water level, and intense rainfall, culminating in massive local river discharge (Perini et al., 2015a, 2015b). Furthermore, according to the classification of Armaroli et al., (2012), the Saint Agatha storm was expected to have a strong impact on the coast, exceeding the combined wave and water level hazard thresholds.

Perini et al. (2015b) reported that the event was forecasted by the regional forecasting chain and the E-R EWS. An alert of Level 1 (out of 3 levels, from 1 to 3) was issued at regional level already on the 4 of February. The following day it was increased to Level 2. The regional protocol allowed to monitor the evolution of the event with the support of measuring stations (i.e. weather, waves, water levels), webcams, waves and surge forecasts and the EWS alerts (updated every day). Damage monitoring began on the 6 of February, consisting of the STBs visiting the impacted locations from the ground while the Civil Protection implemented a first helicopter flight. This flight provided oblique aerial pictures used later to map storm impacts. Two other flights were performed to complete the survey on the 8 and 10 of February. In that period, the SGSS collected on-line material such as pictures, movies and news. All the information was archived in the regional database, although the material is currently not available online. However, information on the storm and its impacts are available at the RISC-KIT Storm Impact Database (http://risckit.cloudapp.net/risckit/#/) (Ciavola et al., 2018).

The whole dataset was used to evaluate the impacts along the coast and the observed ingression line (elaborated from aerial pictures and local measurements, where available) was compared with the risk maps produced for the Floods Directive (2007/60/EC) (Perini et al., 2016). Based on this analysis, Perini et al. (2015b) showed that the inundation extension was similar to the inundation scenario defined by an event with a representative return period of 100 years (e.g. Cesenatico). In specific locations, however, the inundation exceeded the 100 years scenario limit (e.g. Lido di Savio) or aligned with the 10 years flooding scenario.

Severe damages to several concession properties and urban areas were recorded along the coast (Perini et al., 2015a, 2015b). In the Ferrara province, the impacts were mainly confined to the exposed beach, causing significant damage to the concessions (urbanized beaches), to the dune systems (natural areas) and smaller harbours (e.g. flooding of the Porto Canale in Porto Garibaldi). In the Ravenna province, several coastal towns experienced extensive flooding of residential areas (e.g. Lido di Dante, Classe and Savio, where a flood water depth of 2 m was recorded; Perini et al., 2015b).

As part of the quick response effort, the research team performed post-event assessments at several locations in the Ferrara and Ravenna provinces within two weeks after the event. In this work, the analysis of the survey is presented for Lido degli Estensi (i.e. the target area in Figure 1E) in the Ferrara province is shown.

Figure 2. Saint Agatha storm hydrodynamic data including significant wave height (m), wave period (s), direction of waves (nautical degrees), total water level (m), predicted tide (m) and non-tidal residual (m). The start and end time of the storm is referenced to the local storm threshold condition of Hs = 1.5 m and referenced to GMT.

3 Methods

3.1 Quick Response Protocol

A local approach for coastal post-storm field surveys, hereafter called Quick Response Protocol (QRP), was developed and its application within the study area (Section 2) is presented. The approach was implemented by a team of surveyors, know furthermore as the Quick Response Team (QRT), by integrating E-R EWS input, RTK GPS and UAV survey techniques, interviews with local stakeholders, and damage observation. In the framework of the risk management cycle, the QRP is shown in its general form in Figure 3.

Ideally, the response phase of data collection must be activated and completed as soon as possible, prior to initiation of beach recovery processes (natural or human-driven). In this study, the on-line regional forecasting system and the E-R EWS (see Section 2.2) provided guidance to the QRT by indicating the specific coastal areas within the regional domain that were likely to be impacted by the approaching storm and when conditions allowed for safe survey activities on-the-ground and airborne. Thus, the QRT knew prior to the storm impacting the coast where the quick response would most likely be needed and prepared in advance for personnel scheduling and survey equipment.

To detect morphological changes, a base-line of the pre-storm conditions needs to be defined. Typically, the pre-storm survey, consisting of a topo-bathymetric survey through both RTK GPS and UAV techniques, should be performed whenever possible, given enough time and resources. However, it is most critically necessary (i) in case studies where important morphological changes take place over short time-scales and/or (ii) when other sources of information are not available on the pre-storm condition in the likely impacted area. In all other cases, it is possible to assume that the base-line is represented by the most recent available topo-bathymetric dataset, accounting for the limitations linked to this kind of assumption, as it was done for this study (see Section 3.2).

The implementation of the QRP included a number of field activities to acquire both qualitative and quantitative information on the St. Agatha storm in the immediate aftermath of the event. The critical tasks of the approach included the following activities:

- Conduct interviews of citizens, shopkeepers, restaurant owners, and other local stakeholders;
- Annotate the visible damage to coastal defences, buildings, infrastructures;
- Take pictures of the horizontal flood limits and vertical flood marks;
- Map and measure the vertical elevation of flood marks on buildings and defence structures;

- Map the horizontal flood limit;
- Survey of the beach by means of RTK GPS (profiles and control points) and UAV flights.

In this application, the survey tasks focused on the emerged portion of the beach since the UAV system was not capable of measuring bathymetric data in the submerged area. Typically, the RTK GPS technique can be used to survey the intertidal area of the cross-shore profiles at most micro-tidal environments such as this pilot site. This information could be used in comparison with the pre-storm dataset, when covering the same area. However, this data would not be suitable to perform reliable 2D morphological analysis. Possible improvements of this aspect are given in Section 6.

The QRP steps enabled collection of necessary data for an integrated analysis of the storm effects on the coast. The need to conduct rapid field survey activities in this study required the contribution of several people: at least 2 to 3 skilled operators were necessary to accomplish all the tasks in the field, every day. Depending on the alongshore extent and width of the coast that needs to be covered, the implementation of the protocol could last from a few days to a few weeks. In this study, 7 days were sufficient to complete the tasks along a total beach extent of approximately 7 km for the case study site (Figure 1D), resulting in the integrated assessment rate of 1 km per day. In total, 10 profiles and more than 40 flood limits and flood marks were surveyed with RTK GPS technique. Six km of beach were surveyed with the UAV and more than 50 GCPs (Ground Control Points) were surveyed on the ground with the RTK GPS for use in the photogrammetric processing, error analysis and data comparison.

The data processing and analysis of the acquired information is further described in the next sections, focusing on the target area (Figure 1E). The integrated information will help to understand the overall effect of the storm in the surveyed area. The scientific aim of the QRP is to provide useful input to coastal managers for hazard and risk assessment purposes (Figure 3), integrating the post-storm information collected at the regional level.

Figure 3. The Quick Response Protocol in the framework of the Disaster Management Cycle.

3.2 Pre-storm conditions

The pre-storm conditions of the subaerial beach and backshore were assumed to be represented by the available LiDAR-derived DTM from October 2014, with 1x1 m resolution. The dataset was used as reference for the morphological variations of the emerged beach due to the storm impact, as no major events occurred between October 2014 and the Saint Agatha event.

3.3 Stakeholder interviews

Local stakeholders were interviewed by the QRT on the morning of the 7 of February 2015. The interviews were mainly based on informal questions of their recent experiences during the St. Agatha storm. Questions focused on the timing and evolution

of the flood event; what the people were doing before, during and after the event; if they were alerted and prepared. They were also requested to give an interpretation of the causes of the impacts of the event to gauge their education and experience with storm impacts. Ten stakeholders were interviewed in Porto Garibaldi (Figure 1D), the town in the north of Lido degli Estensi. The group included owners of commercial or touristic services (e.g. concessions, restaurants, shops and others), one resident, one fisherman and one fireman. In this work, the interviews were mainly used to understand which local areas were impacted the most, to understand the temporal evolution of the storm impacts, and to better organize the field activities.

3.4 RTK GPS survey

Field measurements relative to flood limits, flood marks, and beach profiles were taken using a RTK GPS (Trimble R6). All measurements were referenced to WGS84 UTM33N coordinates and the national geoid Italgeo99 for elevation. The flood limit denotes the maximum water progression on the plan view and it is evidenced by the presence of objects and debris moved inland by the water during the storm (see Figure 4A). These points are hereafter called "GPS Floodlines" and were mapped with RTK GPS. A flood mark denotes the maximum water depth at a specific location where the water level was clearly visible, for example, walls, buildings, trees or dunes (e.g. Figure 4B). These points, hereafter called "GPS Floodmarks", were associated with a GPS location and a water depth measured with a simple meter (see Figure 4B).

Cross-shore beach profiles were also surveyed to have a comparison (i.e. *a posteriori*) with the post-storm Digital Surface Model (DSM) generated from the UAV photogrammetric analysis (see Section 3.5). Ten cross-shore profiles were measured throughout the surveyed area highlighted in Figure 1D. The measurements were taken on the bare ground and thus excluding variation in the elevation due to debris, wood or other objects. Two profiles belong to the case study target area (Profile 1 and Profile 2 in Figure 1E). These profiles were used to provide a quantification of error (i.e. RMSE) of the UAV processed data.

Figure 4. Examples of "GPS Floodline" (A) and "GPS Floodmark" (B) measurements.

3.5 UAV survey and photogrammetric process

A commercial off-the-shelf UAV, the DJI Phantom Vision 2+, was used to conduct the aerial surveys capturing digital imagery of the pilot case study site. The survey was performed manually in a lawn-mower pattern (e.g. boustrophedon flight pattern) back and forth across the beach. Manual flights were performed as, at the time of the survey, the team did not have at its disposal automatic flight tools and software. This approach influenced the results (as expected) and this aspect will be emphasized and discussed in the following sections. Photos were automatically collected every three seconds from elevations between 40-60 m, at speeds of less than 4 m/s. The UAV camera utilized a fixed focal length and constant exposure. The resulting ground sampling distance and image overlap were estimated to be ~2.5 cm/pixel and ~70%, respectively. The UAV approach enabled surveying of the target area (~0.15 km^2; Figure 1E) within a 10-minute flight collecting more than 550

images. Ground Control Points (GCPs) were measured using an RTK GPS (Trimble R6) for use within the photogrammetric process. The GCPs were selected identifying objects on the beach (e.g. coloured plastic objects, wood or concrete platforms, etc.) that were considered easily detectable from the images. However, the resolution of the acquired images allowed detection of 14 GCPs for the target area (Figure 1E) that were used in the photogrammetric process.

A commercially available photogrammetry software package, specifically Pix4D Pro (Version 3.0.13), was used to stitch the collected UAV photos into one continuous orthomosaic by matching points within overlapping images utilizing Structure-from-Motion (SfM) algorithms. The application of UAV-based SfM photogrammetry for coastal morphology assessment has been recently demonstrated by the studies of Casella et al. (2014; 2016), Turner et al. (2016), Dohner et al. (2016) and Scarelli et al. (2017). The process followed the step-wise procedure illustrated in Figure 5. Images were initially matched using embedded GPS metadata from the UAV, characterized by poor accuracy (few meters). A sparse point cloud was created based on the identified matching points and the calculated initial image camera positions. Then, GCPs were manually identified on the pictures and their GPS information were used to reduce error in georeferencing, as their position was measured with higher accuracy (few centimetres) than the images. A dense point cloud was therefore generated by densification of the corrected sparse cloud. The DSM and orthomosaic were then created from the dense point cloud. The dense cloud was not manually cleaned during the process, meaning that points representing debris, wood or other objects were not removed and therefore included in the final products. This limitation, presented in other published works such as Casella et al. (2014), will be stressed and discussed in the following sections and specific remedies will be proposed in Section 6. The DSM and orthomosaic were then exported for the analysis (see Section 4). A summary of the information of the Pix4D report is given in Table 1 while, the distribution of the GCP vertical errors assessed by the photogrammetric software, is shown in Figure 1E.

Table 1. Pix4D Report Summary.

Keypoints	median of 17344 per image
Calibrated images	581 out of 583
Optimization	Relative difference initial vs optimized parameters: 0.08%
Matches	median of 1198.54 per calibrated image
3D GCPs	14 GCPs; mean RMS error = 0.026 m
Overlapping images for pixel	>5

Figure 5. Sequence of processing steps used in the photogrammetric workflow of UAV images. Main details of each step are given in the dashed boxes.

4 Results

The results of the post-event assessment are presented in the following sections. First, a summary of the interviews is given. Then, the results of the RTK GPS and UAV surveys are presented (and compared) for the target area (Figure 1E) of the pilot case study (Figure 1D).

4.1 Summary of the interviews

Many of the stakeholders reported that the water level inside the Porto Canale of Porto Garibaldi (Figure 1D) was approaching the level of the embankments (~1.8 m above MSL) due to the combined effect of the canal discharge and the sea conditions on the evening of the 5 of February (Thursday). On this same evening, the emerged beaches were impacted by high water levels and waves. The overflow of the canal started between 01:00 and 02:00 GMT and continued till 04:00, mainly because of the oscillations of the water surface following wave propagation inside the canal. Early Friday morning, the situation was still critical, but improved in the early afternoon, when the stormy sea conditions began to subside. Some stakeholders stated they did not remember a similar event in the last 30, 50 or even 60 years.

It became evident to the local people in Porto Garibaldi on the 5 February 2015 that a strong coastal event was approaching their coasts. However, several stakeholders claimed that no clear local alert was issued to the population and none of those interviewed knew about the regional E-R EWS. Basically, local know-how and experiences were their only instruments to understanding and preparing for the situation (e.g. deploying sand bags). They also reported that the Civil Protection arrived at the location on the 6 of February (Friday), at approximately 13:00 GMT, bringing sand bags and assistance.

4.2 Elevation data

An indication of the quality of the DSM produced from the analysis of the UAV images was derived comparing it with the RTK GPS cross-section points (see Figure 1E). The comparison is shown in Figure 6 for both profiles. For both datasets the assumed (i.e. *a priori*) vertical uncertainty is shown, namely ±15 cm for UAV-derived data and ±5 cm for RTK GPS data illustrated by the shaded outlines. Outliers were deleted from the DSM data extracted for Profile 1 and 2 when they were visually determined to be clearly not representative of the terrain surface. However, it was not possible to correct the variations induced by debris or other small objects affecting the DSM in a similar manner and where therefore retained in the surface. Profiles were smoothed using a moving average for the DSM and RTK GPS derived data to reduce noise. The Root Mean Square Errors (RMSEs) of the vertical elevation between the RTK GPS and DSM data were 14 cm and 12 cm for Profiles 1 and 2, respectively. Note that Profile 2 is located in the central portion of the target area, where more precision was expected due to greater image overlap and GCP control targets, while Profile 1 is closer to the edge of the domain where the DSM is expected to be less accurate. Since the DSM data comes from a commercial software and thus relies on GCPs for positioning accuracy, the UAV surveys are therefore not wholly independent of the GPS system. Nevertheless, the UAV-derived DSM provided a useful and efficient dataset alongside the traditional RTK GPS measurements.

This comparison gave an indication of accuracy and reliability of the UAV-derived DSM. The DSM, while overestimating the elevation in the higher portion of the Profile 1, with the strongest difference on the order of 25-30 cm, converged with the RTK GPS profile in the lower portion of Profile 1 near the swash zone. For Profile 2, many of the morphological features were captured, including the storm berm (with a vertical error on the berm top of ~15 cm). The slopes of the emerged foreshore are comparable for both profiles: for Profile 1 the calculated slope was 0.016 for the UAV-derived profile, while it resulted in 0.014 for the RTK GPS profile. The same slopes calculated for Profile 2 resulted in 0.021 and 0.018, respectively. This profile convergence is implemented in further morphological change analysis as shown in Section 4.4.

Thus, the foreshore slope, berm shape, and berm crest locations are well captured by the UAV-derived DSM in Figure 6. The largest disagreement between the DSM and RTK GPS profiles occurs landward of the berm in the back portion of the beach (around 30 cm for Profile 1 and 20 cm for Profile 2). A combination of factors possibly contributed to this difference including lower sampling resolution of the RTK GPS compared to the UAV, manual flight controls which did not maintain constant flight altitude and images overlap, the inclusion of non-terrain elevations such as wood and debris in the DSM, and other affecting factors such as the texture of the beach surface and the position of the sun (see Sections 5 and 6 for the discussion of these limitations and proposed remedies, respectively).

Figure 6. Comparisons between the February 2015 post-storm observed RTK GPS profile survey and post-storm UAV-derived DSM for Profiles 1 and 2. The error bands, defined *a priori* (±15 cm for UAV and ±5 cm for GPS) for visualization purposes, are shown. The RMSE calculated *a posteriori* between the RTK GPS and UAV-derived data are reported.

4.3 Erosion and sedimentation patterns

Erosion and sedimentation patterns are shown in Figure 7. The morphological variations (Figure 7A1, B1 and C1) were obtained from the comparison between the DTM of October 2014 and the post-event UAV-derived DSM. The DSM included non-terrain objects and buildings, thus the analysis of the morphological features only focused on the emerged beach. The results are only presented for the area limited by the GCPs. The inclusion of non-beach features in the DSM, mainly because of the presence of different sized debris, affected the non-uniformity of the shown patterns.

Figure 7A1 shows that the formation of a storm berm is clearly visible running alongshore with a varying width of 20 to 50 m. The vertical deposit is interrupted by erosion scour channels due to water return flows (Figure 7A1). Seaward of the depositional area (i.e. the storm berm) a negative variation pattern highlights the erosion of the ordinary berm, which intensifies just in front of the scour channels (Figure 7A1). Thus, the berm vertically grew and moved landward during the storm as result of sediment transport in the breaker zone (Figure 7A1). At the same time, a small portion of deposition in the intertidal area potentially corresponded to the development of a low tide terrace, at the edge of the analysed domain. However, the domain does not include the lower intertidal area. Therefore, it is not possible to evaluate the morphological variation of the lower

limit of the foreshore. A general lowering landward of the storm berm can be noted (Figure 7A1), which corresponds to the area where the differences between the RTK GPS profiles and the UAV-derived DSM were higher (see Section 4.2 and Figure 6). Thus, this variation can be subjected to error or even representing an artefact. Focusing on the selected frames (Figure 7B, B1, C, C1), visible scour channels are highlighted, which possibly developed along pre-existing footpaths, essentially providing preferential pathways for water retreat seaward following storm conditions. This highlights the UAV's ability to map finer resolution features such as scour channels.

Figure 7. Morphological variations: (A) the UAV-derived orthomosaic of the target area, where morphological features are visible along with the position of the GCPs; (A1) the difference between the post-event UAV-derived DSM and the pre-storm LiDAR-derived DTM. In B, B1 and C, C1 enlargements of the main features are given. The morphological variations are only shown for the area surrounded by the GCPs.

4.4 Coastal flooding

Figure 8 compares the results obtained for the flood extension from the UAV-derived data with the RTK GPS observed flood limits and marks. Flood lines were extracted from the orthomosaic by observing the debris that deposited on the beach defining the main flooded area (i.e. "UAV Floodline" in Figure 8). It was observed that several areas, that were not included in the main flooded areas, were reached by the water through small paths. Those spots, hereby defined "UAV Secondary Flood" areas, are reported in Figure 8.

The agreement seen between the "UAV Floodline" and the RTK GPS derived flood line ("GPS Floodline") can be considered as validation of the orthomosaic. The flooding was mainly limited to the beach in front of the concessions (Figure 8). Some of them, however, experienced secondary flooding where the limit of the flood reached the border of the concessions and the water found a path to flow in to the properties (Figure 8A, B, C, D). These impacts were also observed during the collection of picture and damage observation, but it was not possible to understand the extension of the flooding from the ground, as the private concessions were fenced, and admission was not allowed.

The maximum elevation reached by the water was calculated using the RTK GPS measurements (i.e. "GPS Floodline" and "GPS Floodmark" points) and extracting the elevation of the UAV-derived DSM along the "UAV Floodline". The calculated average elevations reached by the water resulted in 1.634 m and 1.645 m for RTK GPS and UAV data, respectively. The associated standard deviations were 0.079 m and 0.196 m, respectively. The same analysis using the "UAV Floodline" was performed on the pre-storm DTM and it resulted in an average elevation of 1.663 m, with standard deviation equals to 0.093 m. A water depth of 30 cm was measured in the location of the flood mark (Figure 8A).

Figure 8. Observed "GPS Floodline" and "GPS Floodmark" (green and red circles), UAV (red solid line and light-blue polygons) flood extension comparisons: the box on the left shows an overview of the target area while on the right (A, B, C and D) some spot-focuses are given.

5 Discussion

In this section the results are discussed, along with their limitations, with focus on the summary of the local interviews and the comparisons between RTK GPS and UAV-derived data. A focus on the integration of the regional assessment with the local information is given.

5.1 Interviews

Interviews with local stakeholders provided details on what happened during the night between the 5 and the 6 of February 2015 (see Section 4.1). The evolution of the St. Agatha storm described by people was consistent with the observed hydrodynamic data (see Section 2.3 and Figure 2). The interviews focused on impacts in Porto Garibaldi, which were mainly caused by the overflow of the canal harbour. However, the interviewed could give indications on the surrounding impacted areas (i.e. Lido degli Estensi and Spina) and thereby helping the research team to better organize the field activities. An interesting aspect highlighted through interviews was a lack of alerts notifications to the population concerning the approaching storm. However, coastal managers reported that several alerts were issued before the event to municipalities and Civil Protection agencies (Perini et al., 2015b). The fact that the Civil Protection reached the location only on 6 of February (Friday), after the peak of the event, supports the hypothesis that, even if the alert was issued from the regional to the municipality level, there was a communication problem between the regional and local managers, the emergency proactive responders, and the local population. This was also indirectly confirmed by the interviewed fireman who claimed that they were not even prepared to act on coastal locations. It appeared that the population of the area was not aware of the on-line E-R EWS platform, where alerts and warnings could be readily found. These aspects support the idea that more effort should be spent improving the preparedness and response of the Civil Protection and the awareness of the local population, especially through improvement of communication channels and local coastal risk knowledge. These aspects were also reported by Martinez et al. (2018), about the same event and the same locations, in the wider framework of the aims of the EU FP7 RISC-KIT Project (GA 603458; www.risckit.eu) (Van Dongeren et al., 2018). Pescaroli and Magni (2015) also highlighted the importance of this aspects based on the analysis of local community interviews in Cesenatico (Figure 1C). The limitations of the interviews presented here are mainly related to the lack of a standardized methodology, as the questions were mainly informal, and a limited number of people involved. A standard approach (e.g. using prepared questionnaire) can produce more relevant information that can be statistically analysed, when the number of interviewed is large enough. Several examples of methodological approaches for stakeholder interviews and analysis of their outcomes exist in the literature, for diverse purposes, that could be adapted to be applied during a post-storm assessment (Pescaroli and Magni, 2015; Becu et al., 2017; Gray et al., 2017; Martinez et al., 2018).

5.2 RTK GPS and UAV-derived data

RMSEs of 14 and 12 cm between the DSM and RTK GPS data (see Section 4.2 and Figure 6) are similar for both analysed profiles and comparable with the LiDAR-derived data uncertainty. In comparison with error estimates of UAV products reported by recent studies, the resulting RMSE values of the DSM compared to the RTK GPS profile surveys are comparable (Casella, 2014 and 2016; Dohner et al., 2016) or higher (Turner et al., 2016; James et al., 2017; Scarelli et al., 2017). The low accuracy of the DSM product is attributed to aspects related to both the field implementation and the photogrammetric process. A recent study by James et al. (2017) provides practical suggestions to improve the quality of the field survey (e.g. modifications to UAV flight characteristics, the number and spacing of GCPs, etc.). Overall DSM improvement is achieved through increased image overlap, that can be properly controlled with automated flights constraining the variability of the flight altitude as well. GCPs play a major role in the quality of the photogrammetric products, as increased DSM accuracy of one order of magnitude occurs when properly used (e.g. Moloney et al., 2017). In addition, the UAV-derived DSM should only be considered valid in the area limited by the GCPs. The number, position and accuracy of the measured GCPs detectable from the images are thus extremely important. In this application, the selected GCPs (i.e. 14 GCPs for 0.15 km^2) were not uniformly distributed and, because of the ground sampling distance, not always detectable from the images. Following Seymour et al. (2017), it is possible to assume that the inaccuracy of the final product can be also due to the (combined effect of the) homogeneous texture of the beach surface and the high position of the sun during the flight (that in this study was performed at 12:00 GMT). Overexposure and smooth (in elevation and colour) surfaces can indeed undermine the SfM processing. Regarding the photogrammetric reconstruction, non-terrain objects (i.e. human structures and debris) were not removed or filtered from the point cloud during processing and remained in the dataset as was seen also in a similar storm response study by Casella et al. (2014). Thus, objects such as wood, litter and buildings, locally affected the represented surface. This, consequently, influenced the comparison with the post-storm RTK GPS observations, which only represented the terrain surface. The quality of the products can be further improved (see Section 6 for proposed improvements), however, the DSM was still able to capture key morphologic features (i.e. storm berm and scour channels).

The morphological patterns (see Section 4.3) derived from the UAV data gave an opportunity to assess the morphological response of the beach at a detailed resolution. The results showed the erosion of the ordinary berm and the formation of a storm berm. The scouring channels highlighted in Figure 7 were potentially triggered by the presence of concrete pathways concentrating and accelerating the return water flow during the waning phase of the storm. To reduce the formation of these scouring channels and the consequent worsening of beach erosion, a reasonable option would be to remove, or at least retreat landward, the pathways during the winter season (Nordstrom et al., 2015). The level of detail of the outcomes suggests that it is possible to use UAV-derived products to calculate volume variations, as already confirmed by the literature on the topic (e.g. Turner et al., 2016).

The UAV-derived orthomosaic offered a rapid, accurate approach to mapping the flood extension (see Section 4.4). The general agreement with the RTK GPS on-the-ground observations confirmed the close geopositioning of the images and

provided a validation of the assessed flood extension. The opportunity to observe the flood extension from the UAV data made it possible to define a detailed and continuous flood line. To obtain the same results with a RTK GPS survey, the operator should increase the point sampling (or even use a continuous sampling method). This prolongs the field activities on the beach and increases operational costs. Also, the aerial point of view is essential to having a complete view of the flood line evolution while, from the RTK GPS viewpoint, the random distribution and spreading of the debris can mislead the operator. The maximum elevations reached by the water, separately assessed considering RTK GPS measurements and the UAV-derived data, were comparable (~1.65 m), although the second one was characterized by higher uncertainty. As the maximum total water level measured during the storm was 1.20 m (P. Corsini tide gauge, Figure 1C; see Section 2.3), a component of ~0.45 due to wave run-up and set-up must be considered for the water to reach the estimated average elevations on the emerged beach. This value is comparable to the same component calculated using the formula proposed by Suanez et al. (2015) for storm conditions (i.e. 0.40 m and 0.53 m, respectively), considering the average slopes of 0.015 and 0.02 (which are representative of those calculated for the Profiles 1 and 2 analyzed in this study, see Section 4.1) and the hydrodynamics of the storm (see Section 2.3). On the other hand, it is lower than the component calculated with the traditional formula by Stockdon et al. (2006), which resulted in 1.14 m for both slopes (i.e. dissipative conditions). To improve the number and detail of mapped flood marks it is possible, during the survey, to use the UAV system to collect oblique aerial images of specific (urban and non-urban) flooded areas to derive 3D dense clouds, following the approach proposed by Giordan et al. (2018). Indeed, the dense cloud can be analysed to retrieve, measure and map morphological evidences of the water level on dunes or building facades.

5.3 Local and regional assessments

Compared to the post-storm regional assessment reported in Perini et al. (2015b), based on the analysis of oblique aerial images collected from a helicopter (see Sections 2.2 and 2.3), the proposed survey approach for local assessments can produce very detailed and accurate data. Indeed, the flood ingression extracted from the dataset of Perini et al. (2015b) is not as accurate and detailed as the information that can be capture with UAVs flying at ~50 m altitude. Moreover, the regional analysis of the flood ingression was not implemented in this case study because the Civil Protection flight was performed too late, when the markers of the limit of the inundation were no longer identifiable from the helicopter (Armaroli C., personal communication). Thus, a direct comparison between the two observed flood extensions was not possible. It was possible, however, to compare the "UAV Floodline" with the regional flood maps (T10 and T100; Perini et al., 2016). This comparison is shown in Figure 9, for the target area. In this location, the inundation extension was less than the one calculated for the 10 years return period event (T10). This is in contrast with the evidences of Perini et al. (2015b) highlighted at regional level (see Section 2.3) and, specifically, for the two reported examples of Cesenatico and Lido di Savio that showed more similarity with the 100 years (T100) and the less frequent (>100 years) scenarios, respectively. This difference can be attributed to the fact that the regional maps are calculated with a static approach, not grounded in process-based formulas or models, applying a constant total water level (1.49 m and 1.81 m for T10 and T100, respectively) at the shoreline and propagating the inundation with a modified

bathtub-based approach (i.e. including cost-distance and damping effects as surrogates of hydrodynamics), over a 2 m resolution LiDAR DTM from 2008 (more details in Perini et al., 2016). Thus, site specific processes (e.g. wave run-up and set-up) are not properly considered, potentially leading to the differences highlighted above. This hypothesis is also supported by the fact that the assessed maximum elevation reached by the water is close to the average between the levels used to calculate the T10 and T100 scenarios. Therefore, the observed flood line should have been located between the T10 and T100 flood limits.

Regarding the morphological analysis, the variations captured from the UAV can be used to calculate more accurate volume changes, at local level, than those calculated on representative beach profiles along the coast. The regional approach indeed focuses only on a limited number of beach profiles along the coast.

The regional protocol does not include any attempt to involve local communities through interviews or other methods as the STBs, activated after the event, mainly collect qualitative information through direct observations and pictures (see Section 2.2). This represents a serious limitation of the regional approach that could benefit by involving the local coastal communities in the assessment.

5.4 Towards an integrated multi-scale assessment framework

Nowadays, several techniques are available for coastal surveys providing various types of maps and models. In many cases, different sensors can provide similar products. As example, very high-resolution orthomosaics can be produced with UAVs. Laser scanners can provide 3D coloured dense point clouds that can be used to derive such kind of products, while with RTK GPS and LiDAR systems this is not possible. To understand what the best approach is, efficiency in the field must be considered. Indeed, the level of detail of the shown UAV-derived products as well as the efficiency of field surveying make the presented approach highly effective for post-storm assessment when compared with pure RTK GPS or terrestrial laser scanner-based approaches, as confirmed by the literature. For example, Moloney et al. (2017) estimated that to complete the survey (including set-up time) of the same area (i.e. a coastal dune test area of 85 m x 65 m) the RTK GPS technique required ~13.45 hours, the laser scanner ~3.66 hours, while the UAV only ~1.15 hours. The field efficiency of the UAV was also higher (10^4 and 25 times faster than the RTK GPS and laser scanner ones, respectively) in terms of rate of measured points per hours. Even considering that RTK GPS surveys can be completed by 1 skilled person, while the UAV needs 2-3 people as does the laser scanner, the proposed approach results in more efficient and comprehensive data acquisition. Focusing on costs, adopting low-cost UAVs such as the one used in this study or in Moloney et al. (2017) and a licensed photogrammetric software, the RTK GPS survey method is less expensive. However, the higher costs of UAV-based surveys are balanced by the efficiency and the speed of the field activities. It must be noted that, the UAV platform used for this study needs additional data collected with a GPS RTK system.

Considering (i) the above-mentioned advantages of UAV-based approaches for surveying; (ii) the benefits of a more social-based approach that provides detailed, local information important for the proper organization of the field tasks and the assessment; and (iii) the limitations of the regional-scale assessments highlighted in Section 5.3; it is conceivable that

procedures adopted at the regional level can be improved with local actions to provide more reliable and detailed information. In this sense, the proposed QRP can be very helpful to integrating and completing the regional protocol for post-storm assessment with more local, qualitative, and quantitative information. It is advisable to integrate local protocols (such as the QRP) in the regional one through adoption of UAV-based and social-based approaches. As the regional authorities do not have sufficient manpower and instruments to perform such local detailed assessments along the whole coast, the proposed approach can be performed at local level by academic and private survey teams (such as the QRT), activated similar to STBs (see Section 2.2), after the coastal event. By properly organizing the efforts at different locations on the coast (i.e. the most impacted areas), it will be possible to activate a quick, multi-scale, coordinated protocol in the immediate aftermath of an event acting at regional and local levels. This will provide more holistic data coverage, and increase the details and reliability of the assessments, as demonstrated by Giordan et al. (2018) proposing and testing a multi-scale, multi-sensor approach for riverine flood assessments. That study provided a multi-step framework successfully combining satellite data collected before, during and after the event, with post-event aerial, UAV and RTK GPS surveys for flood and damage mapping ranging from the regional, basin, and local scales. The framework represents a good example, from the methodological point of view, on how to integrate datasets collected at different scales.

Figure 9. Comparisons between the observed "UAV Floodline" and the flood scenarios (T10 and T100) computed by Perini et al. (2016).

6 Suggestions for possible improvements

In order to improve the data quality, the following suggestions are presented and should be implemented in the QRP.

The use of automatic flight planning will considerably improve the quality of the survey though controlled flight altitude and image overlap. To perform such local scale assessments, ground sampling distances from 2 to 5 cm/pixel should be obtained (e.g. Giordan et al., 2018) and images captured with overlap ~70-80% (e.g. Dohner et al., 2016; Turner et al., 2016). The UAV survey should be planned on a larger domain (~10% buffer) than needed for data collection as edges have lower image overlap, higher uncertainty, and potential data loss.

The GCPs should be uniformly distributed throughout the survey domain and near boundaries to prevent skewing within the DSM product. The GCPs should be easily detectable, considering the ground sampling distance, as playing an important role in maximizing the accuracy of photogrammetric products. This depends on both the quality of the images (related to the camera system, the type, flight speed, and altitude of the flight) and of the type of GCPs. An example of GCPs used during the survey can be found in Figure 10 with images of good (A, B) and poor (C, D) quality targets. Proper GCPs can be prepared using flat wood panels painted with two contrasting colours (e.g. red/white, yellow/black). In this case, however, the surveyors must bring them in the filed while in this application the GCPs were selected using objects found on the beach. On the ground,

photos of GCP locations should be taken to have the idea of exactly where the RTK GPS points were taken on the target objects and within the context of the survey domain.

As suggested in Section 5, environmental conditions (e.g. texture of the beach surface and sun conditions; Seymour et al., 2017) can influence the accuracy of the products and the operators should consider these aspects when planning the field activities.

The photogrammetric process can also be improved, for example, by spending more effort in cleaning and filtering the point cloud, thus minimizing the effect of debris and others on the final products.

The post-storm survey did not include the submerged area. To extend the protocol to this part of the beach, other innovative approaches should be adopted, such as near-shore low-cost autonomous surface systems (e.g. Hampson et al., 2011). However, it is beyond the aim of this work to include these aspects in the protocol.

Qualitative observations and interviews are also significant and should be performed as soon as possible and as detailed as possible during the implementation of the QRP. It is important to adopt standard approaches for stakeholder involvement and interview a large number of people in order to allow statistical analysis of qualitative information and increase representativeness.

The larger the number of surveyors involved in the post-event survey, the faster the data can be the collected. In addition, the team can be divided into groups with specific tasks (e.g. performing interviews, RTK GPS or UAV surveys, etc.), speeding up the survey process. Planning the activities is crucial for efficient and high-quality performance of the QRT. This can be supported by activities completed during the non-storm season, such as instrument maintenance and preparation, monitoring of the warning system performances, tasks planning and assignment, etc.

To provide more accurate qualitative flooding and morphologic results (see Section 5), further analyses should be performed. This paper only presents the analysis of a small portion (Figure 1E) of the whole case study (Figure 1D) and deeper investigations (e.g. including forcing, sediment and volume change analysis, possibly supported by numerical models; including more detailed socio-economic aspects for precise impact assessments; etc.) are needed to provide more robust hazard and risk assessments. However, the QRP has been demonstrated to be a proper approach to quickly assess the storm effects at local level in the immediate aftermath of an event, through its combination of technologies and planning approaches. Thus, in the framework of coastal management (Figure 3), a proper application of the QRP can produce useful information that can be used at local, regional and national levels in order to: (i) update hazard and risk maps; (ii) provide detailed information for flood-damage curves calibration (see, as example, the study of Scorzini and Frank, 2017); and (iii) provide insights for risk mitigation and management plans. Finally, as suggested in Section 5, the QRP can be integrated in regional protocols, improving the reliability of the regional hazard and risk assessments.

Figure 10. Photos A and B at the top demonstrate practical GCPs based on unique shapes, colors, and ability to see from a high altitude. Photos C and D, on the bottom, demonstrate error-inducing GCPs due to their height off the ground and indistinguishable shape, size, and color in aerial images.

7 Conclusions

This case study illustrates the potential and benefits of an integrated approach combining UAVs with on the ground RTK GPS surveys and qualitative data collection through stakeholders' interviews for coastal storm impact assessments at local level. The presented protocol was applied at a pilot case study in the Emilia-Romagna coast, after the impact of an extreme coastal storm. Results were presented and discussed, for demonstration purposes, on a small portion of the pilot case study site.

As a general remark, (i) interviewing local stakeholders and people in charge of emergency response tasks are extremely useful for supporting the field activity organization, as well as at detecting lacks in the alert chain, preparedness, and response emergency phases; (ii) the UAV approach was found to be effective for erosion and flooding assessments, by providing detailed, continuous and two (and three)-dimensional information, with less time spent in the field in comparison with traditional RTK GPS surveys and other approaches.

The main limitation of the analysis of the interviews was due to the lack of a standardized approach, that should be adopted and adapted from the literature. The main limitation of the UAV products was linked to field implementation and lacks in the photogrammetric process. Specific suggestions for improvements were given, such as the use of automated flights, proper GCPs and the cleaning of the point cloud during the photogrammetric process.

Regarding the proposed QRP, further applications can directly support hazard and impact assessment at local and regional levels, and thus addressing coastal management needs. Indeed, the outcomes of the analysis were compared with the post-event assessment performed by the regional authorities highlighting that the proposed protocol for local assessment can be readily integrated in the regional ones, improving the accuracy and reliability of the regional assessments.

Competing interests

The authors declare that they have no conflict of interest.

Acknowledgements

E. Duo and P. Ciavola were supported by the EU FP7 RISC-KIT ("Resilience-increasing Strategies for Coasts – Toolkit"; GA 603458; www.risckit.eu) project during field activities and data analysis, and the EU H2020 ANYWHERE (EnhANcing emergencY management and response to extreme WeatHER and climate Events; GA 700099; www.anywhere-h2020.eu) project during the manuscript preparation and review process. The work was facilitated by a sabbatical grant to A. Trembanis. Acquisition and utilization of the UAV system was made possible through funding from the UNIDEL foundation and from NOAA Sea Grant project NOAA SG-2016-18 RRCE-8 TREMBANIS. The authors are also thankful to Clara Armaroli, Duccio

Bertoni, Mohammad Muslim Uddin, and Sarah Trembanis for their help on gathering data in the field and to Marc Sanuy, Ap Van Dongeren and Tom Spencer for their valuable comments and suggestions during the preparation of the manuscript.

References

Anderson, K. and Gaston, K. J.: Lightweight unmanned aerial vehicles will revolutionize spatial ecology, Front. Ecol. Environ., 11(3), 138–146, doi:10.1890/120150, 2013.

Armaroli, C. and Duo, E.: Validation of the coastal storm risk assessment framework along the Emilia-Romagna coast, Coast. Eng., 134, 159-167, doi:10.1016/j.coastaleng.2017.08.014, 2018.

Armaroli, C., Ciavola, P., Masina, M. and Perini, L.: Run-up computation behind emerged breakwaters for marine storm risk assessment, J. Coast. Res., SI 56 (Proceedings of the 10th International Coastal Symposium, Lisbon, Portugal), 1612–1616, available at: http://www.jstor.org/stable/25738062, 2009.

Armaroli, C., Ciavola, P., Perini, L., Calabrese, L., Lorito, S., Valentini, A. and Masina, M.: Critical storm thresholds for significant morphological changes and damage along the Emilia-Romagna coastline, Italy, Geomorphology, 143–144, 34–51, doi:10.1016/j.geomorph.2011.09.006, 2012.

ARPA E-R SIMC: Rapporto dell'evento meteorologico del 5 e 6 febbraio 2015, Bologna, available at: http://www.arpa.emr.it/cms3/documenti/_cerca_doc/meteo/radar/rapporti/Rapporto_meteo_20150205-06.pdf, 2015.

Bason, C., Jacobs, A., Howard, A. and Tymes, M.: White Paper on the Status of Sudden Wetland Dieback in Saltmarshes of the Delaware Inland Bays, Delaware Department of Natural Resources and Environmental Control, available at: http://www.dnrec.delaware.gov/Admin/DelawareWetlands/Documents/swdwhitepaper07final.pdf, 2007.

Becu, N., Amalric, M., Anselme, B., Beck, E., Bertin, X., Delay, E., Long, N., Marilleau, N., Pignon-Mussaud, C. and Rousseaux, F.: Participatory simulation to foster social learning on coastal flooding prevention, Environ. Model. Softw., 98, 1–11, doi:10.1016/j.envsoft.2017.09.003, 2017.

Benedet, L., Finkl, C. W. and Hartog, W. M.: Processes Controlling Development of Erosional Hot Spots on a Beach Nourishment Project, J. Coast. Res., 23(1), 33–48, doi:10.2112/06-0706.1, 2007.

Berni, J. A. J., Zarco-Tejada, P. J., Suárez, L. and Fereres, E.: Thermal and Narrowband Multispectral Remote Sensing for Vegetation Monitoring From an Unmanned Aerial Vehicle, IEEE Trans. Geosci. Remote Sens., 47(3), 722–738, doi:10.1109/TGRS.2008.2010457, 2009.

Bernstein, D. J., Freeman, C., Forte, M. F., Park, J.-Y., Gayes, P. T. and Mitasova, H.: Survey design analysis for three-dimensional mapping of beach and nearshore morphology, in: Proceedings of the International Conference on Coastal Sediments 2003, Clearwater Beach, Florida, USA (18–23 May 2003), edited by R. A. Davis, A. Sallenger, and P. Howd, World Scientific, 2003.

Billi, P. and Rinaldi, M.: Human impact on sediment yield and channel dynamics in the Arno River basin (central Italy), in: Human Impacts on Erosion and Sedimentation: Proceedings of Rabat Symposium S6, Rabat, Morocco, 23 April - 3 May 1997, edited by D. E. Walling and J.-L. Probst, pp. 301–311, International Association of Hydrological Sciences, 1997.

Bush, D. M., Neal, W. J., Young, R. S. and Pilkey, O. H.: Utilization of geoindicators for rapid assessment of coastal-hazard risk and mitigation, Ocean Coast. Manag., 42(8), 647–670, doi:10.1016/S0964-5691(99)00027-7, 1999.

Casella, E., Rovere, A., Pedroncini, A., Mucerino, L., Casella, M., Cusati, L. A., Vacchi, M., Ferrari, M. and Firpo, M.: Study of wave runup using numerical models and low-altitude aerial photogrammetry: A tool for coastal management, Estuar. Coast. Shelf Sci., 149, 160–167, doi:10.1016/j.ecss.2014.08.012, 2014.

Casella, E., Rovere, A., Pedroncini, A., Stark, C. P., Casella, M., Ferrari, M. and Firpo, M.: Drones as tools for monitoring beach topography changes in the Ligurian Sea (NW Mediterranean), Geo-Marine Lett., 36(2), 151–163, doi:10.1007/s00367-016-0435-9, 2016.

Ciavola, P., Ferreira, O., Haerens, P., Van Koningsveld, M. and Armaroli, C.: Storm impacts along European coastlines. Part 2: Lessons learned from the MICORE project, Environ. Sci. Policy, 14(7), 924–933, doi:10.1016/j.envsci.2011.05.009, 2011.

Ciavola, P., Harley, M. D. and Den Heijer, C.: The RISC-KIT storm impact database: A new tool in support of DRR, Coast. Eng., 134, 24-32, doi:10.1016/j.coastaleng.2017.08.016, 2018.

Dohner, S. M., Trembanis, A. C. and Miller, D. C.: A tale of three storms: Morphologic response of Broadkill Beach, Delaware, following Superstorm Sandy, Hurricane Joaquin, and Winter Storm Jonas, Shore & Beach, 84(4), 2016.

Giordan, D., Notti, D., Villa, A., Zucca, F., Calò, F., Pepe, A., Dutto, F., Pari, P., Baldo, M., and Allasia, P.: Low cost, multiscale and multi-sensor application for flooded area mapping, Nat. Hazards Earth Syst. Sci., 18, 1493–1516, https://doi.org/10.5194/nhess-18-1493-2018, 2018.

Gray, J. D. E., O'Neill, K. and Qiu, Z.: Coastal residents' perceptions of the function of and relationship between engineered and natural infrastructure for coastal hazard mitigation, Ocean Coast. Manag., 146, 144–156, doi:10.1016/j.ocecoaman.2017.07.005, 2017.

Hampson, R., MacMahan, J. and Kirby, J. T.: A Low-Cost Hydrographic Kayak Surveying System, J. Coast. Res., 27(3), 600–603, doi:10.2112/JCOASTRES-D-09-00108.1, 2011.

Hansen, J. E. and Barnard, P. L.: Sub-weekly to interannual variability of a high-energy shoreline, Coast. Eng., 57(11–12), 959–972, doi:10.1016/j.coastaleng.2010.05.011, 2010.

Harley, M. D., Valentini, A., Armaroli, C., Perini, L., Calabrese, L. and Ciavola, P.: Can an early-warning system help minimize the impacts of coastal storms? A case study of the 2012 Halloween storm, northern Italy, Nat. Hazards Earth Syst. Sci., 16(1), 209–222, doi:10.5194/nhess-16-209-2016, 2016.

Harley, M., Valentini, A., Armaroli, C., Ciavola, P., Perini, L., Calabrese, L. and Marucci, F.: An early warning system for the on-line prediction of coastal storm risk on the Italian coastline, in: Coastal Engineering 2012 Proceedings of 33rd Conference on Coastal Engineering, Santander, Spain, 1-6 July 2012, edited by P. Lynett and J. M. Smith, Coastal Engineering Research Council, doi:10.9753/icce.v33.management.77, 2012.

James, M. R., Robson, S. and Smith, M. W.: 3-D uncertainty-based topographic change detection with structure-from-motion photogrammetry: precision maps for ground control and directly georeferenced surveys, Earth Surf. Process. Landforms, 42(12), 1769–1788, doi:10.1002/esp.4125, 2017.

Jiménez, J. A., Armaroli, C. and Bosom, E.: Preparing for the Impact of Coastal Storms: A Coastal Manager-Oriented Approach, in: Coastal Storms: Processes and Impacts, edited by P. Ciavola and G. Coco, pp. 217–239, John Wiley & Sons Ltd., 2017.

Larson, M. and Kraus, N. C.: Temporal and spatial scales of beach profile change, Duck, North Carolina, Mar. Geol., 117(1–4), 75–94, doi:10.1016/0025-3227(94)90007-8, 1994.

Lee, G.-H., Nicholls, R. J. and Birkemeier, W. A.: Storm-driven variability of the beach-nearshore profile at Duck, North Carolina, USA, 1981-1991, Mar. Geol., 148(3–4), 163–177, doi:10.1016/S0025-3227(98)00010-3, 1998.

Lee, J.-M., Park, J.-Y. and Choi, J.-Y.: Evaluation of Sub-aerial Topographic Surveying Techniques Using Total Station and RTK-GPS for Applications in Macrotidal Sand Beach Environment, J. Coast. Res., SI 65 (Proceedings 12th International Coastal Symposium, Plymouth, England), 535–540, doi:10.2112/SI65-091.1, 2013.

Ligorio, C., Primerano, S., Strocchi, M. and Beghelli, E. (Eds.): Il sistema regionale di allertamento per il rischio idrogeologico-idraulico, Regione Emilia-Romagna and Agenzia Regionale di Protezione Civile, Bologna, Italy, 2012.

Mancini, F., Dubbini, M., Gattelli, M., Stecchi, F., Fabbri, S. and Gabbianelli, G.: Using Unmanned Aerial Vehicles (UAV) for High-Resolution Reconstruction of Topography: The Structure from Motion Approach on Coastal Environments, Remote Sens., 5(12), 6880–6898, doi:10.3390/rs5126880, 2013.

Martinez, G., Armaroli, C., Costas, S., Harley, M. D. and Paolisso, M.: Experiences and results from interdisciplinary collaboration: Utilizing qualitative information to formulate disaster risk reduction measures for coastal regions, Coast. Eng., 134, 62-72, doi:10.1016/j.coastaleng.2017.09.010, 2018.

Masina, M. and Ciavola, P.: Analisi dei livelli marini estremi e delle acque alte lungo il litorale ravennate, Studi Costieri, 18, 87–101, available at: http://www.gnrac.unifi.it/rivista/Numero18/Articolo6.pdf, 2011.

Mendoza, E. T. and Jiménez, J. A.: Storm-Induced Beach Erosion Potential on the Catalonian Coast, J. Coast. Res., SI 48 (Proceedings of the 3rd Spanish Conference on Coastal Geomorphology, Las Palmas de Gran Canaria, Spain), 81–88, available at: http://www.jstor.org/stable/25737386, 2006.

Mendoza, E. T., Jiménez, J. A. and Mateo, J.: A coastal storms intensity scale for the Catalan sea (NW Mediterranean), Nat. Hazards Earth Syst. Sci., 11(9), 2453–2462, doi:10.5194/nhess-11-2453-2011, 2011.

Moloney, J. G., Hilton, M. J., Sirguey, P., and Simons-Smith, T.: Coastal Dune Surveying Using a Low-Cost Remotely Piloted Aerial System (RPAS), J. Coast. Res., in press, https://doi.org/10.2112/JCOASTRES-D-17-00076.1, 2017.

Morton, R. A., Leach, M. P., Paine, J. G. and Cardoza, M. A.: Monitoring Beach Changes Using GPS Surveying Techniques, J. Coast. Res., 9(3), 702–720, doi:10.2307/4298124, 1993.

Morton, R. A.: Factors Controlling Storm Impacts on Coastal Barriers and Beaches-A Preliminary Basis for for near Real-Time Forecasting, J. Coast. Res., 18(3), 486–501, available at: http://www.jstor.org/stable/4299096, 2002.

Nicholls, R. J., Wong, P. P., Burketts, J. O., Codignotto, J. E., McLean, R. F., Ragoonaden, S. and Woodroffe, C. D.: Coastal systems and low-lying areas, in: Climate Change 2007: Impacts, Adaptation and Vulnerability. Contribution of Working Group II to the Fourth Assessment Report of the Intergovernmental Panel on Climate Change, edited by M. L. Parry, O. F. Canziani, J. P. Palutikof, P. J. Van Der Linden, and C. E. Hanson, pp. 315–356, Cambridge University Press, Cambridge, UK, 2007.

Nordstrom, K. F., Armaroli, C., Jackson, N. L. and Ciavola, P.: Opportunities and constraints for managed retreat on exposed sandy shores: Examples from Emilia-Romagna, Italy, Ocean Coast. Manag., 104, 11–21, doi:10.1016/j.ocecoaman.2014.11.010, 2015.

Pawlowicz, R., Beardsley, B. and Lentz, S.: Classical tidal harmonic analysis including error estimates in MATLAB using T_TIDE, Comput. Geosci., 28(8), 929–937, doi:10.1016/S0098-3004(02)00013-4, 2002.

Perini, L., Calabrese, L., Lorito, S. and Luciani, P.: Costal flood risk in Emilia-Romagna (Italy): the sea storm of February 2015, in: Coastal and Maritime Mediterranean Conference, Edition 3, Ferrara, Italy, 25-27 November 2015, edited by D. Levacher, M. Sanchez, P. Ciavola, and E. Raymond, pp. 225–230, Editions Paralia, doi:10.5150/cmcm.2015.044, 2015a.

Perini, L., Calabrese, L., Lorito, S. and Luciani, P.: Il rischio da mareggiata in Emilia-Romagna: l'evento del 5-6 Febbraio 2015, il Geologo, 53, 8–17, available at: http://www.geologiemiliaromagna.it/il-geologo-anno-xv-2015-n-53/, 2015b.

Perini, L., Calabrese, L., Salerno, G., Ciavola, P. and Armaroli, C.: Evaluation of coastal vulnerability to flooding: Comparison of two different methodologies adopted by the Emilia-Romagna region (Italy), Nat. Hazards Earth Syst. Sci., 16(1), 181–194, doi:10.5194/nhess-16-181-2016, 2016.

Perini, L., Luciani, P. and Calabrese, L.: Altimetria della fascia costiera, in: Il sistema mare-costa dell'Emilia-Romagna, edited by L. Perini and L. Calabrese, pp. 57–66, Regione Emilia-Romagna, Bologna, Italy, 2010.

Pescaroli, G. and Magni, M.: Flood warnings in coastal areas: How do experience and information influence responses to alert services?, Nat. Hazards Earth Syst. Sci., 15(4), 703–714, doi:10.5194/nhess-15-703-2015, 2015.

Phillips, M. S., Blenkinsopp, C. E., Splinter, K. D., Harley, M. D., Turner, I. L. and Cox, R. J.: High-frequency observations of berm recovery using a continuous scanning Lidar, in Australasian Coasts & Ports 2017: Working with Nature, pp. 872–878, Barton ACT: Engineers Australia, PIANC Australia and Institute of Professional Engineers New Zealand, 2017.

Pietro, L. S., O'Neal, M. A. and Puleo, J. A.: Developing Terrestrial-LIDAR-Based Digital Elevation Models for Monitoring Beach Nourishment Performance, J. Coast. Res., 24(6), 1555–1564, doi:10.2112/07-0904.1, 2008.

Poljanšek, K., De Groeve, T., Marín Ferrer, M. and Clark, I. (Eds.): Science for disaster risk management 2017: knowing better and losing less, Publications Office of the European Union, Luxembourg, doi:10.2788/688605, 2017.

Preciso, E., Salemi, E. and Billi, P.: Land use changes, torrent control works and sediment mining: Effects on channel morphology and sediment flux, case study of the Reno River (Northern Italy), Hydrol. Process., 26(8), 1134–1148, doi:10.1002/hyp.8202, 2012.

Sanuy, M., Duo, E., Jäger, W.S., Ciavola, P., and Jiménez, J.A.: Linking source with consequences of coastal storm impacts for climate change and risk reduction scenarios for Mediterranean sandy beaches, Nat. Hazards Earth Syst. Sci., 18, 1825–1847, https://doi.org/10.5194/nhess-18-1825-2018, 2018.

Saye, S. E., Van der Wal, D., Pye, K. and Blott, S. J.: Beach-dune morphological relationships and erosion/accretion: An investigation at five sites in England and Wales using LIDAR data, Geomorphology, 72(1–4), 128–155, doi:10.1016/j.geomorph.2005.05.007, 2005.

Scarelli, F. M., Sistilli, F., Fabbri, S., Cantelli, L., Barboza, E. G. and Gabbianelli, G.: Seasonal dune and beach monitoring using photogrammetry from UAV surveys to apply in the ICZM on the Ravenna coast (Emilia-Romagna, Italy), Remote Sens. Appl. Soc. Environ., 7, 27–39, doi:10.1016/j.rsase.2017.06.003, 2017.

Scorzini, A. R. and Frank, E.: Flood damage curves: new insights from the 2010 flood in Veneto, Italy, J. Flood Risk Manag., 10(3), 381–392, doi:10.1111/jfr3.12163, 2017.

Seymour, A.C., Ridge, J.T., Rodriguez, A.B., Newton, E., Dale, J., and Johnston, D.W.: Deploying Fixed Wing Unoccupied Aerial Systems (UAS) for Coastal Morphology Assessment and Management, J. Coast. Res., in press, https://doi.org/10.2112/JCOASTRES-D-17-00088.1, 2017.

Stockdon, H. F., Holman, R. A., Howd, P. A., and Sallenger, A. H.: Empirical parameterization of setup, swash, and runup, Coast. Eng., 53(7), 573-588, https://doi.org/10.1016/j.coastaleng.2005.12.005, 2006.

Stockdon, H. F., Sallenger Jr., A. H., List, J. H. and Holman, R. A.: Estimation of Shoreline Position and Change Using Airborne Topographic Lidar Data, J. Coast. Res., 18(3), 502–513, doi:10.2307/4299097, 2002.

Stone, G. W., Liu, B., Pepper, D. A. and Wang, P.: The importance of extratropical and tropical cyclones on the short-term evolution of barrier islands along the northern Gulf of Mexico, USA, Mar. Geol., 210(1–4), 63–78, doi:10.1016/j.margeo.2004.05.021, 2004.

Suanez, S., Cancouët, R.,Floc'h, F., Blaise, E., Ardhuin, F., Filipot, J.-F., Cariolet, J.-M., and Delacourt, C.: Observations and Predictions of Wave Runup, Extreme Water Levels, and Medium-Term Dune Erosion during Storm Conditions, J. Mar. Sci. Eng., 3, 674-698; doi:10.3390/jmse3030674, 2015.

Swales, A.: Geostatistical estimation of short-term changes in beach morphology and sand budget, J. Coast. Res., 18(2), 338–351, available at: http://www.jstor.org/stable/4299079, 2002.

Sytnik, O. and Stecchi, F.: Disappearing coastal dunes: tourism development and future challenges, a case-study from Ravenna, Italy, J. Coast. Conserv., 19(5), 715–727, doi:10.1007/s11852-014-0353-9, 2015.

Taramelli, A., Di Matteo, L., Ciavola, P., Guadagnano, F. and Tolomei, C.: Temporal evolution of patterns and processes related to subsidence of the coastal area surrounding the Bevano River mouth (Northern Adriatic) - Italy, Ocean Coast. Manag., 108, 74–88, doi:10.1016/j.ocecoaman.2014.06.021, 2015.

Teatini, P., Ferronato, M., Gambolati, G., Bertoni, W. and Gonella, M.: A century of land subsidence in Ravenna, Italy, Environ. Geol., 47(6), 831–846, doi:10.1007/s00254-004-1215-9, 2005.

Theuerkauf, E. J. and Rodriguez, A. B.: Impacts of Transect Location and Variations in Along-Beach Morphology on Measuring Volume Change, J. Coast. Res., 28(3), 707–718, doi:10.2112/JCOASTRES-D-11-00112.1, 2012.

Trembanis, A., Duval, C., Beaudoin, J., Schmidt, V., Miller, D. and Mayer, L.: A detailed seabed signature from Hurricane Sandy revealed in bedforms and scour, Geochemistry, Geophys. Geosystems, 14(10), 4334–4340, doi:10.1002/ggge.20260, 2013.

Turner, I. L., Harley, M. D. and Drummond, C. D.: UAVs for coastal surveying, Coast. Eng., 114, 19–24, doi:10.1016/j.coastaleng.2016.03.011, 2016.

Van Dongeren, A., Ciavola, P., Martinez, G., Viavattene, C., Bogaard, T., Ferreira, Ó., Higgins, R. and McCall, R.: Introduction to RISC-KIT: Resilience-increasing strategies for coasts, Coast. Eng., 134, 2-9, doi:10.1016/j.coastaleng.2017.10.007, 2018.

Viavattene, C., Jiménez, J. A., Ferreira, O., Priest, S., Owen, D. and McCall, R.: Selecting coastal hotspots to storm impacts at the regional scale: A Coastal Risk Assessment Framework, Coast. Eng., 134, 33-47, doi:10.1016/j.coastaleng.2017.09.002, 2018.

Westoby, M. J., Brasington, J., Glasser, N. F., Hambrey, M. J. and Reynolds, J. M.: "Structure-from-Motion" photogrammetry: A low-cost, effective tool for geoscience applications, Geomorphology, 179, 300–314, doi:10.1016/j.geomorph.2012.08.021, 2012.

Young, A. P. and Ashford, S. A.: Performance Evaluation of Seacliff Erosion Control Methods, Shore & Beach, 74(4), 16–24, 2006.

Captions

Figure 1. Field study site locations: A) Emilia-Romagna region; B) Coastal regional domain; C) Locations of the nearest tide gauge and wave buoy; D) Pilot case study site; E) Target area for data comparison.

Figure 2. Saint Agatha storm hydrodynamic data including significant wave height (m), wave period (s), direction of waves (nautical degrees), total water level (m), predicted tide (m) and non-tidal residual (m). The start and end time of the storm is referenced to the local storm threshold condition of Hs = 1.5 m and referenced to GMT.

Figure 3. The Quick Response Protocol in the framework of the Disaster Management Cycle.

Figure 4. Examples of "GPS Floodline" (A) and "GPS Floodmark" (B) measurements.

Figure 5. Sequence of processing steps used in the photogrammetric workflow of UAV images. Main details of each step are given in the dashed boxes.

Figure 6. Comparisons between the February 2015 post-storm observed RTK GPS profile survey and post-storm UAV-derived DSM for Profiles 1 and 2. The error bands, defined *a priori* (±15 cm for UAV and ±5 cm for GPS) for visualization purposes, are shown. The RMSE calculated *a posteriori* between the RTK GPS and UAV-derived data are reported.

Figure 7. Morphological variations: (A) the UAV-derived orthomosaic of the target area, where morphological features are visible along with the position of the GCPs; (A1) the difference between the post-event UAV-derived DSM and the pre-storm LiDAR-derived DTM. In B, B1 and C, C1 enlargements of the main features are given. The morphological variations are only shown for the area surrounded by the GCPs.

Figure 8. Observed "GPS Floodline" and "GPS Floodmark" (green and red circles), UAV (red solid line and light-blue polygons) flood extension comparisons: the box on the left shows an overview of the target area while on the right (A, B, C and D) some spot-focuses are given.

Figure 9. Comparisons between the observed "UAV Floodline" and the flood scenarios (T10 and T100) computed by Perini et al. (2016).

Figure 10. Photos A and B at the top demonstrate practical GCPs based on unique shapes, colors, and ability to see from a high altitude. Photos C and D, on the bottom, demonstrate error-inducing GCPs due to their height off the ground and indistinguishable shape, size, and color in aerial images.

Table 1. Pix4D Report Summary.

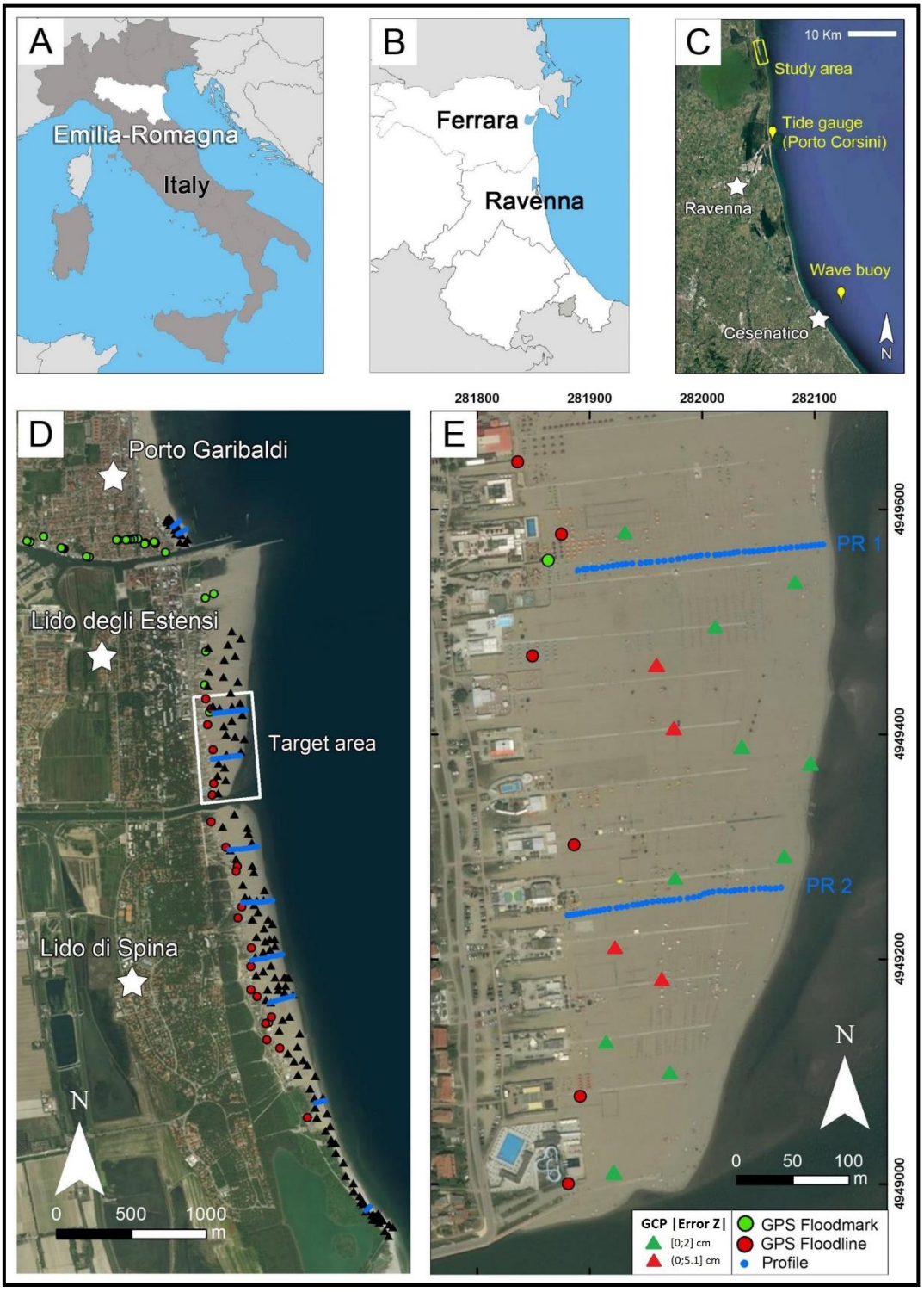
A
Emilia-Romagna
Italy
B
Ferrara
Ravenna
C
10 Km
Study area
Tide gauge
(Porto Corsini)
Ravenna
Wave buoy
Cesenatico
N
D
Porto Garibaldi
Lido degli Estensi
Target area
Lido di Spina
N
0
500
1000
m
E
281800
281900
282000
282100
4949600
4949400
4949200
4949000
PR 1
PR 2
N
0
50
100
m
GCP |Error Z|
[0;2] cm
(0;5.1] cm
GPS Floodmark
GPS Floodline
Profile

Figure 1.

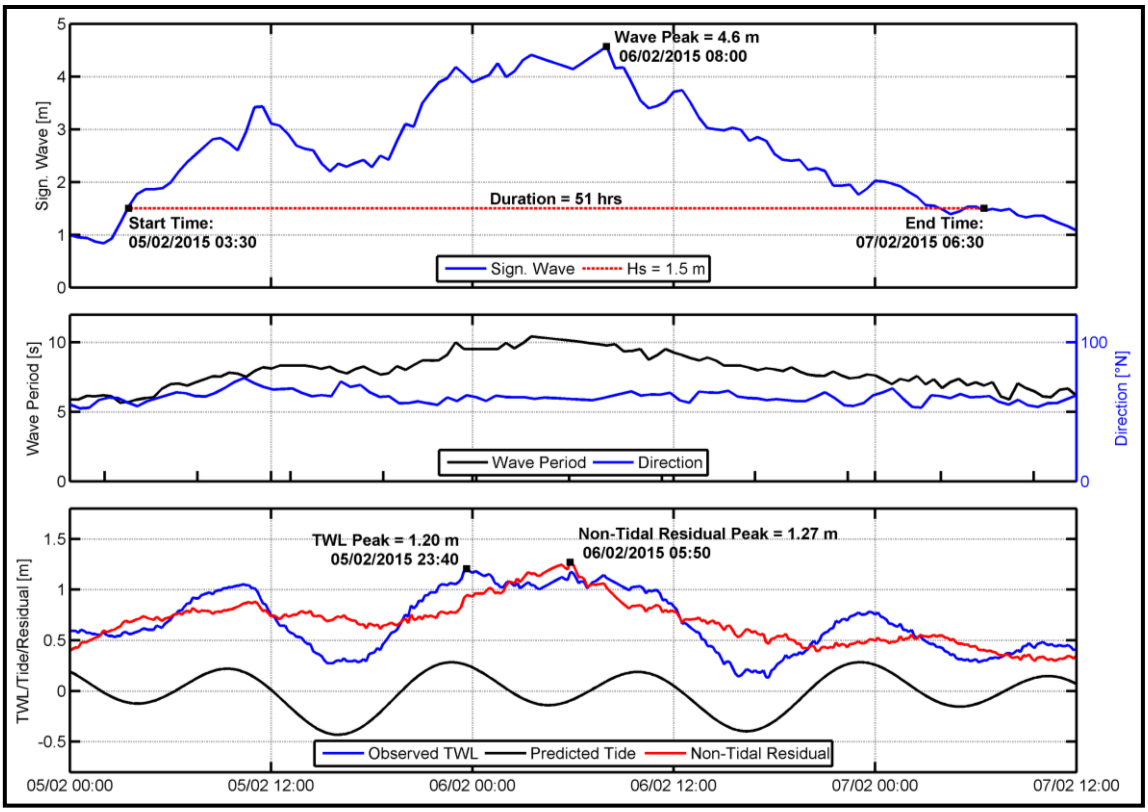
Wave Peak = 4.6 m
06/02/2015 08:00
Sign. Wave [m]
Duration = 51 hrs
Start Time:
05/02/2015 03:30
End Time:
07/02/2015 06:30
Sign. Wave
Hs = 1.5 m
Wave Period [s]
Direction [°N]
Wave Period
Direction
TWL Peak = 1.20 m
05/02/2015 23:40
Non-Tidal Residual Peak = 1.27 m
06/02/2015 05:50
TWL/Tide/Residual [m]
Observed TWL
Predicted Tide
Non-Tidal Residual
05/02 00:00
05/02 12:00
06/02 00:00
06/02 12:00
07/02 00:00
07/02 12:00

Figure 2.

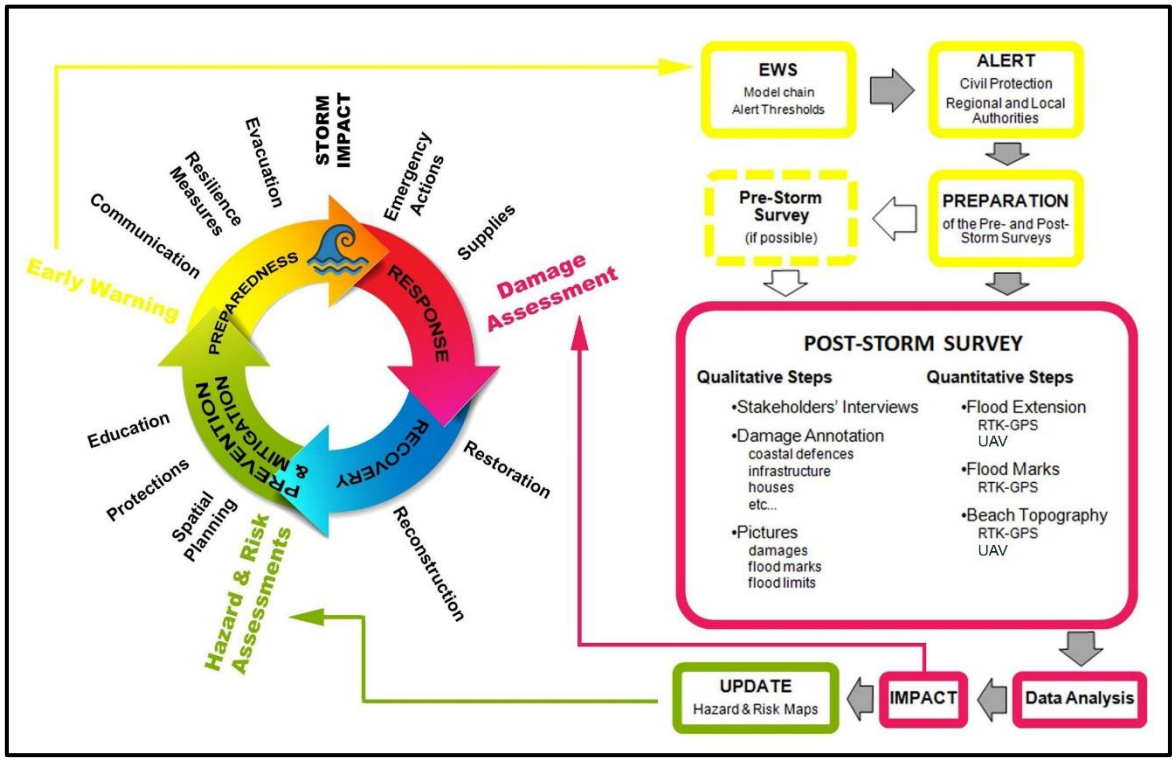
EWS
Model chain
Alert Thresholds
ALERT
Civil Protection
Regional and Local Authorities
Pre-Storm Survey
(if possible)
PREPARATION
of the Pre- and Post-Storm Surveys
POST-STORM SURVEY
Qualitative Steps
•Stakeholders' Interviews
•Damage Annotation
coastal defences
infrastructure
houses
etc...
•Pictures
damages
flood marks
flood limits
Quantitative Steps
•Flood Extension
RTK-GPS
UAV
•Flood Marks
RTK-GPS
•Beach Topography
RTK-GPS
UAV
Data Analysis
IMPACT
UPDATE
Hazard & Risk Maps
STORM IMPACT
Evacuation
Emergency Actions
Supplies
Damage Assessment
Restoration
Reconstruction
Hazard & Risk Assessments
Spatial Planning
Protections
Education
Resilience Measures
Communication
Early Warning
PREPAREDNESS
RESPONSE
RECOVERY
PREVENTION & MITIGATION

Figure 3.

Figure 4.

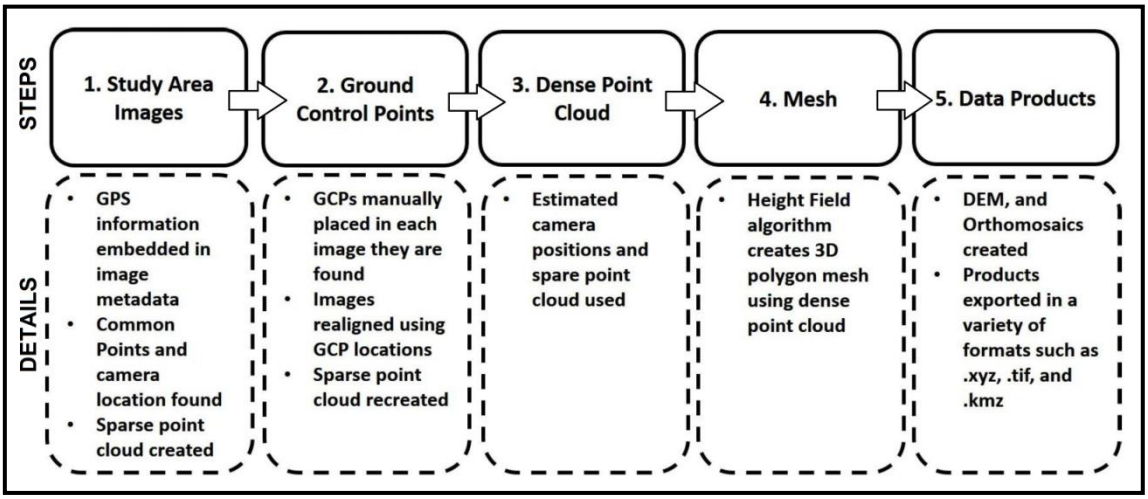
STEPS
1. Study Area Images
2. Ground Control Points
3. Dense Point Cloud
4. Mesh
5. Data Products
DETAILS
GPS information embedded in image metadata
Common Points and camera location found
Sparse point cloud created
GCPs manually placed in each image they are found
Images realigned using GCP locations
Sparse point cloud recreated
Estimated camera positions and spare point cloud used
Height Field algorithm creates 3D polygon mesh using dense point cloud
DEM, and Orthomosaics created
Products exported in a variety of formats such as .xyz, .tif, and .kmz

Figure 5.

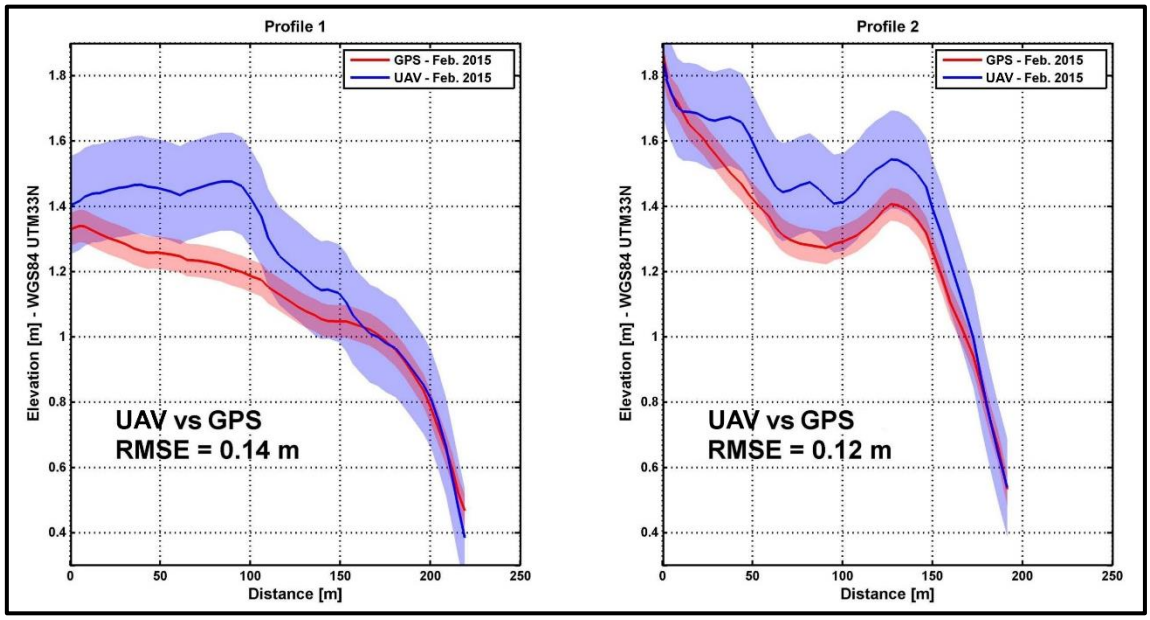
Profile 1
GPS - Feb. 2015
UAV - Feb. 2015
Elevation [m] - WGS84 UTM33N
Distance [m]
UAV vs GPS
RMSE = 0.14 m
Profile 2
GPS - Feb. 2015
UAV - Feb. 2015
Elevation [m] - WGS84 UTM33N
Distance [m]
UAV vs GPS
RMSE = 0.12 m

Figure 6.

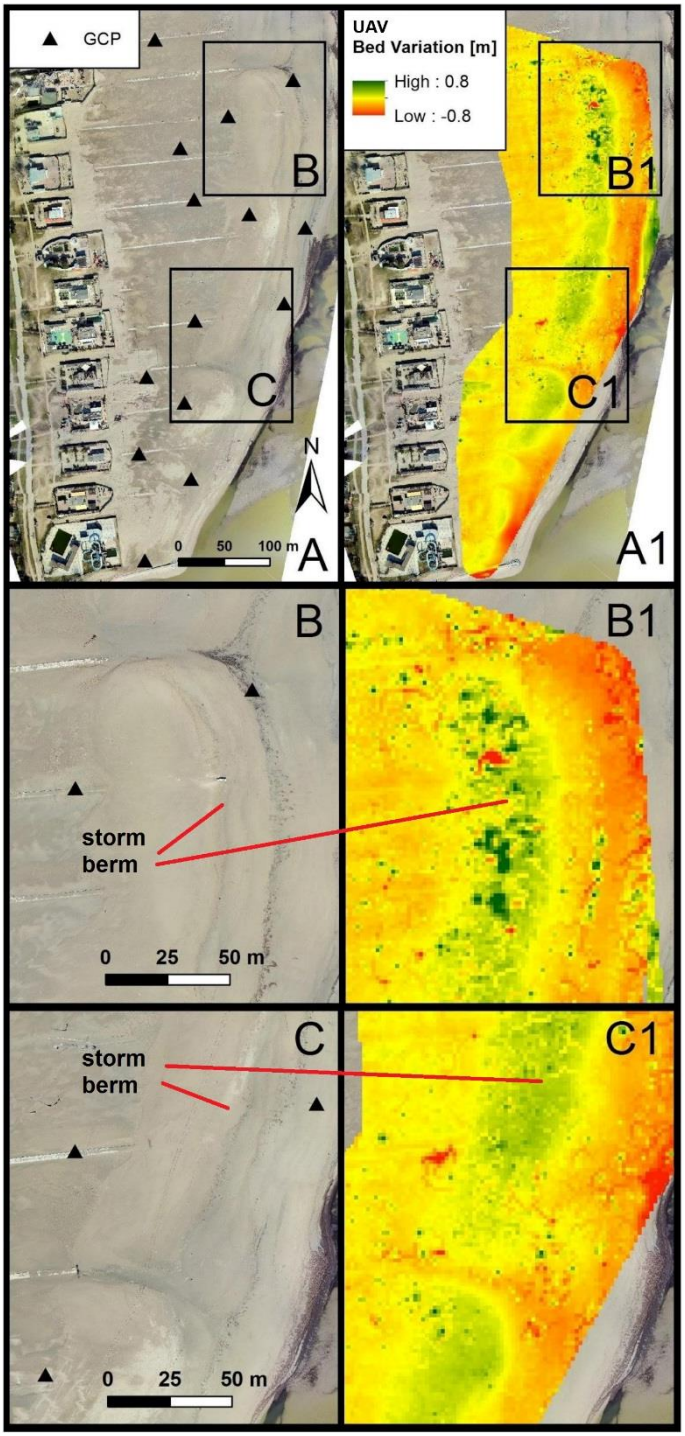
GCP
UAV
Bed Variation [m]
High : 0.8
Low : -0.8
B
C
B1
C1
N
0 50 100 m
A
A1
B
B1
storm
berm
0 25 50 m
C
C1
storm
berm
0 25 50 m

Figure 7.

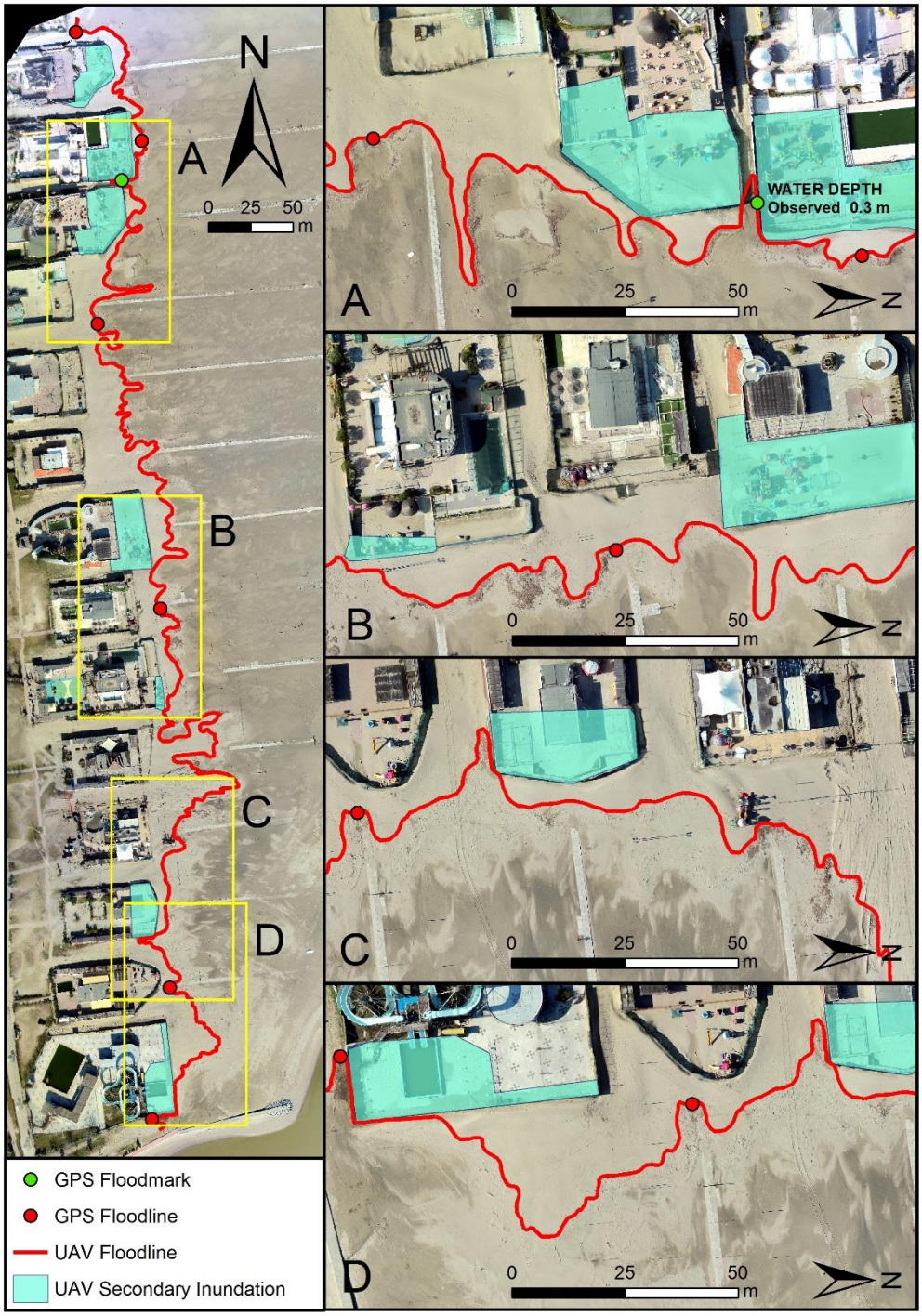
N
A
0 25 50
m
B
C
D
GPS Floodmark
GPS Floodline
UAV Floodline
UAV Secondary Inundation
WATER DEPTH
Observed 0.3 m
A
B
C
D
0 25 50
m
N

Figure 8.

Figure 9.

Figure 10.

Table 1.

Keypoints	median of 17344 per image
Calibrated images	581 out of 583
Optimization	Relative difference initial vs optimized parameters: 0.08%
Matches	median of 1198.54 per calibrated image
3D GCPs	14 GCPs; mean RMS error = 0.026 m
Overlapping images for pixel	>5